

# Airborne Boost-Phase Ballistic Missile Defense

Dean A. Wilkening

---

Boost-phase ballistic missile defense is alluring because rocket boosters are easy to detect and track, they are relatively vulnerable due to the large axial loads on a missile under powered flight, the entire payload (single or multiple warheads and midcourse penetration aids) may be destroyed in a single shot, and countermeasures to defeat boost-phase defense are more difficult to devise than for midcourse ballistic missile defenses. Moreover, if intercepted several seconds before booster burnout, the debris will land well short of the target area, although collateral damage to other territory is a serious concern.

On the other hand, boost-phase ballistic missile defense is technically challenging because the intercept timelines are very short (1–3 minutes for theater-range ballistic missiles and 3–5 minutes for intercontinental range missiles) and missile boosters are accelerating targets, thus complicating the design of homing kinetic-kill vehicles (KKVs). This article examines the technical feasibility and nominal capability of one type of boost-phase defense, namely, airborne boost-phase intercept (ABI). Airborne laser systems are not examined here.<sup>1</sup> This article concludes that ABI should be technically achievable within the next decade and that airborne platforms offer some unique advantages, especially for theater ballistic missile defense, that warrant their serious consideration in future U.S. missile defense architectures.

The advantages of boost-phase ballistic missile defense animated President Reagan's Strategic Defense Initiative. However, unlike boost-phase defense against Russian ICBMs, boost-phase defense against emerging ballistic-missile states does not necessarily require space-based weapons due to their small

---

Received 11 June 2003; accepted 17 December 2003.

Address correspondence to Dean A. Wilkening, Encina Hall, Stanford University, Stanford, CA 94305. E-mail: wilkening@stanford.edu

**Dean A. Wilkening**, Center for International Security and Cooperation, Stanford University, Stanford, CA.

geographic size. Ground, naval, and airborne platforms carrying boost-phase interceptor missiles with intercept ranges on the order of 400 to 700 km can get close enough to get an effective shot. This is important because, while terrestrial boost-phase systems may be effective against ICBMs launched from small states such as North Korea, they would not be effective against ICBMs launched from large countries such as Russia and China, or against submarine-launched ballistic missiles (SLBMs) launched from the open oceans, for the simple reason that they cannot get close enough to all possible Russian or Chinese launch locations to pose a realistic threat. Consequently they would not provoke the kind of negative response from Russia or China that one would expect with space-based boost-phase defenses. In fact, terrestrial boost-phase defenses pose little threat to the strategic forces of any of the five major nuclear powers, thus creating possibilities for collaboration between these states.

Boost-phase intercept systems require a sensor architecture for rapid target detection and tracking, KKV's designed to intercept accelerating ballistic missile targets, interceptor missiles to launch these KKV's at high speeds, and launch platforms to carry the interceptors. Direct collision between the KKV and ballistic missile body destroys the booster, thus rapidly terminating its thrust and possibly destroying the warhead(s) as the booster collapses—although the latter cannot be proved. Consequently, from a defense conservative perspective, one should assume that the payload could be viable. To ensure that the ballistic missile debris, possibly including a live warhead, cannot reach defended territory, intercepts must occur before the payload has sufficient speed to reach this territory typically several seconds to several tens of seconds before booster burnout, depending on the target missile's trajectory.

Soon after a ballistic missile is launched, the sensor architecture detects the event and begins to track the target to obtain a firing solution for the interceptor missile. Rapid launch detection and tracking maximizes the interceptor flight time and, hence, the intercept range. Initially, the interceptor and its KKV are guided using in-flight target updates from external sensors. As soon as the KKV reaches an altitude at which its multi-spectral seeker can begin to operate (above approximately 80 km), it should be able to track the target missile's bright plume. When the KKV approaches to within approximately 100 km of its target (about 10 seconds prior to intercept), the KKV sensors should be able to discriminate the missile hard body from the rocket exhaust plume. An onboard laser imaging, detection and ranging (LIDAR) system would help with the plume-missile hard body track handoff as well as provide accurate range information to improve KKV guidance allowing the aimpoint on the target to be located with an accuracy of approximately 50 cm.<sup>2</sup>

The desired speed and mass of the KKV determines the size of the interceptor missile and, hence, the feasible launch platforms (satellites, aircraft, ships, or ground-based launchers). ABI speeds around 5 km/sec are desirable for both theater and national missile defense. Slower speeds produce short intercept ranges, thus increasing the number of ABI platforms required to cover a particular country and, hence, the system cost. Two-stage missiles with speeds between 5–6 km/sec and masses below 1,500 kg can be designed with current technology. Larger airborne missiles could be designed, but they would not fit easily aboard existing heavy bombers or other large aircraft, much less fighter aircraft or unmanned aerial vehicles (UAVs).

The analysis of boost-phase intercept systems is complex because of the interdependence of different elements in the system, thus requiring design iterations. This analysis strives to be conservative with respect to ABI performance estimates, yet includes systems that are not in existence today but could be deployed within a decade if they significantly impact the effectiveness of boost-phase missile defense, for example, a notional space-based infrared sensor similar to the Space-Based Infra-Red System-High Earth Orbit (SBIRS-High) and powerful airborne X-band radars. The elements of an airborne boost-phase intercept system are examined in detail in this analysis, along with the nominal ABI capability against theater-range and intercontinental-range ballistic missiles. Ballistic missile target characteristics are clearly important for determining ABI effectiveness. Appendix A provides technical details for the ballistic missile targets examined in this study.

## **SENSOR ARCHITECTURE**

Boost-phase intercept requires prompt launch detection and rapid, accurate tracking to launch and guide the interceptor in flight until the KKV can home autonomously on the target. While initial detection and tracking can come from infrared or radar sensors, combining both creates a more robust architecture because it helps eliminate false alarms and makes simple booster decoys more difficult to build because they must mimic radar and optical signatures. Figure 1 illustrates these sensor options. Although detailed sensor architecture designs are quite complicated, their basic limitations, especially with respect to rapid launch detection and tracking, can be understood by examining the physics of each sensor type.

### **Infrared Detection and Tracking**

Passive infrared systems can detect missile plumes with reasonable accuracy from a distance of thousands of kilometers and, hence, can detect ballistic

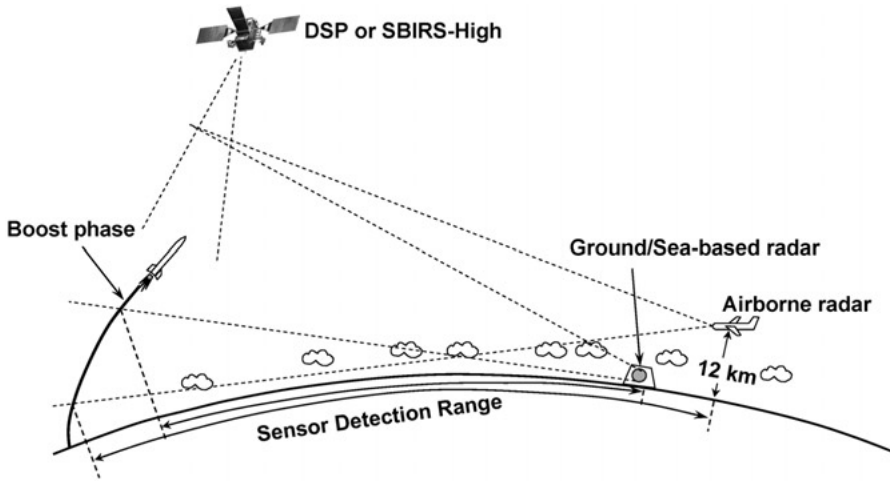


Figure 1: Schematic sensor architecture.

missile launches globally from high-earth or geosynchronous orbits. Space-based and airborne infrared sensors may both be attractive, the former because of their global coverage and the latter because of their high accuracy.<sup>3</sup> However, passive infrared sensors require triangulation from multiple sensors to obtain an accurate track because range information is not available.<sup>4</sup>

Infrared detection and tracking ranges depend on the infrared signal emitted by the target or the reflectance of the target for LIDAR systems, the diameter of the optics, and the minimal detectable signal of the focal plane array, which is a function of the noise in the sensor and signal clutter returns from other objects (e.g., clouds) in the sensor's field of view. Sensor noise is determined by the detector dark current (which is a sensitive function of its temperature) and by blackbody radiation from any warm surfaces in the optical path. It is measured in terms of a Noise Equivalent Intensity (NEI). The precision with which an infrared sensor can determine the missile booster position is determined by the diffraction limit of the optics or the pixel dimensions of the focal plane array, whichever is larger, unless one invokes sub-pixel resolution techniques.

The infrared signal from a rocket plume is a complex function of the altitude of the booster, the engine thrust, and the type of propellant. The infrared signature is produced by optical transitions from excited states of the combustion products—principally water, carbon dioxide, and carbon monoxide. In addition, liquid-propellant boosters produce soot due to the fuel-rich mixtures used to optimize their specific impulse. When heated, soot adds blackbody radiation

to the plume's signature. Similarly, solid-propellant boosters often have metal oxides (e.g., aluminum oxide) added to improve their specific impulse. These solid particles are ejected from the nozzle upon combustion and, like soot, add blackbody radiation to the plume.

As a missile rises in the atmosphere, unburned fuel and combustion products like carbon monoxide and molecular hydrogen continue to burn when mixed with atmospheric oxygen—referred to as “afterburning.” The infrared intensity from large intercontinental ballistic missile plumes is approximately 1–10 MW/sr- $\mu\text{m}$  at their peak intensity, that is, when the missile is at altitudes below 40 km. When the missile's forward speed is close to the exhaust velocity of the combustion products, mixing with atmospheric oxygen occurs more slowly and, hence, the “afterburning” signature drops significantly, leading to a “trough” region in the plume intensity. The “trough” region is typically two to three orders of magnitude less intense than the “afterburning” region and occurs when the missile is at an altitude of approximately 40 km to 60 km. As the missile continues to accelerate, the relative speed of the exhaust plume and the surrounding air again becomes appreciable and the plume signature increases due to more effective mixing and, hence, combustion of the exhaust products. At high altitudes, the oxygen concentration in the atmosphere becomes too low to support significant afterburning and the plume intensity drops again. At altitudes above 100 km the plume expands to such an extent that it often exceeds the field of view of a single sensor pixel, causing a further drop in apparent signal intensity. Staging events also reduce the observed signal because of the smaller thrust for second and third stage rocket motors. Eventually, the plume signature drops to that of the “intrinsic core,” which is the infrared signal one observes directly behind the nozzle from heated exhaust products expanding into the vacuum of outer space. The “intrinsic core” is two to three orders of magnitude less intense than the peak “afterburning” signature. Typical infrared intensities for the intrinsic core for ICBM-class engines are on the order of several hundred to several thousand Watts per steradian per micron.<sup>5</sup>

Infrared ballistic missile early-warning satellites such as the Defense Support Program (DSP) and its future replacement, SBIRS-High, are candidates for missile detection and tracking. The Space-Based Infra-Red System-Low Earth Orbit (SBIRS-Low) is not expected to play a significant role in boost-phase defense because its multi-spectral optical system, particularly its long-wave infrared sensor, is designed to accurately track objects against the cold background of outer space and, hence, cannot observe missiles until relatively late in their boost phase. Moreover, due to significant cost overruns, it is not clear when SBIRS-Low will be deployed, if ever.

DSP operates in the 2.7  $\mu\text{m}$  water absorption band and has a pixel footprint of approximately 1 km  $\times$  1 km on the surface of the earth. This infrared band

was selected because this wavelength is strongly attenuated in the atmosphere, thereby greatly reducing the background signal from spurious infrared sources and clutter returns on or near the surface of the earth. In this band, scattered light from high-altitude clouds is the dominant source of clutter. However, the infrequent DSP revisit rate (approximately 10 sec) introduces detection delays and, therefore, makes this sensor unattractive for booster tracking.

Detecting the launch of a large rocket using space-based infrared sensors is relatively easy for high-thrust ICBM and theater-range ballistic missile first stages. For example, a 300 km-range Scud B missile has the same thrust and, hence, the same intrinsic core intensity as a Minuteman III third-stage rocket motor, that is, about 200 W/sr in the 2.6–2.8  $\mu\text{m}$  band. Such a plume would produce a signal-to-noise ratio of 1 at geosynchronous orbit for a sensor with 30 cm diameter optics and a NEI of  $1 \times 10^{-14}$  W/cm<sup>2</sup>, that is, a signal that is detectable but requires modest integration times to achieve reasonable detection probabilities.<sup>6</sup> However, the signal from a Scud B or Scud C missile as it passes through the afterburning region is hundreds to thousands of times brighter than the intrinsic core and, hence, can be detected by space-based infrared sensors at geosynchronous altitudes, as in fact occurred with DSP during Operation Desert Storm.

This analysis assumes that a sensor like SBIR-High will be deployed to support boost-phase ballistic missile defense. The capability of a notional space-based infrared system like SBIRS-High has been examined in a recent American Physical Society (APS) study.<sup>7</sup> This detector consists of a 30 cm telescope with a HgCdTe focal plane array that stares at 1/24 of the Earth's surface every 33 msec, thus scanning the entire surface in less than one second unless it focuses intentionally on a narrow region of high interest. The APS study assumed that this sensor operated in one of the infrared atmospheric windows (e.g., 2.0–2.5  $\mu\text{m}$  or 3.5–5  $\mu\text{m}$ ) as opposed to an infrared absorption band like DSP, thereby allowing the sensor to see down to the Earth's surface under clear conditions, with a 1 km  $\times$  1 km pixel footprint at the Earth's surface.

Under these circumstances, the latest time at which a notional space-based infrared sensor can detect missile boosters is determined by the presence of optically thick clouds. The APS study concluded that large ballistic missile plumes could be detected with high confidence by a space-based infrared sensor operating in one of the atmospheric windows once the missile reaches an altitude of approximately 7 km.<sup>8</sup> This sets an upper limit on the time delay from missile launch to first detection. Table 1 shows the time it takes for the missiles examined in this study to reach an altitude of 7 km along lofted trajectories. Lofted trajectories have been chosen because, although they can be detected a few seconds earlier, they require more time to develop an accurate track

**Table 1:** SBIR/radar ballistic missile detection and tracking times.

Missile	Boost time (sec)	Burnout altitude (km)	Time to detect <sup>a</sup> (sec)		Time to track (sec)		Total launch delay (sec)		Total interceptor flight time (sec)		
			SBIR (1 km)	Airborne radar	SBIR (1 km)	Airborne radar	SBIR (1 km)	Airborne radar	SBIR (1 km)	Airborne radar	
<b>North Korean launches</b>											
Scud B	61	23-31	33	14 <sup>c</sup>	10	5	43	19	8	10	34
Scud C	85	26-60	37	21 <sup>c</sup>	13	5	50	26	9	26	50
No Dong	95	42-88	35	21 <sup>c</sup>	13	5	48	26	10	37	59
Taeпо Dong 1	165	110-170	43	27 <sup>c</sup>	13	5	56	32	13	96	120
Taeпо Dong 2	193	180-240	39	27 <sup>c</sup>	13	5	52	32	15	126	146
290 sec ICBM	290	185-445	52	44 <sup>c</sup>	13	5	65	49	20	205	221
240 sec ICBM	240	135-440	39	30 <sup>c</sup>	9	5	48	35	17	175	188
180 sec ICBM	180	75-370	32	24 <sup>c</sup>	5	5	37	29	14	129	137
<b>Iranian launches</b>											
Shahdb 3	95	65-75	34	21 <sup>c</sup>	11	5	45	26	10	40	59
Shahdb 4	165	125-170	43	32	14	5	57	37	13	95	115
Shahdb 5	199	180-280	40	45	13	5	53	50	15	131	134
290 sec ICBM	290	185-395	52	60	14	5	66	65	20	204	205
240 sec ICBM	240	145-395	39	45	9	5	48	50	17	175	173
180 sec ICBM	180	85-325	32	37	5	5	37	42	14	129	124

<sup>a</sup>Determined by when the missile reaches 7 km altitude for space-based infrared sensors and when the missile passes into the radar fan (0.42° grazing angle) and has a Doppler shift above 150 km/hr for the airborne radar.

<sup>b</sup>Intercepts are assumed to occur at a time before burn out (TBO) equal to 5 percent of the missile's boost time plus 5 seconds.

<sup>c</sup>Assuming the airborne radar is within 400 km of the launch site.

using space-based infrared sensors and because ABIs have shorter intercept ranges against them due to the need to climb to higher intercept altitudes. Therefore, when these factors are included, lofted trajectories represent worst-case trajectories for boost-phase intercept.

After detection, it takes some time for space-based infrared sensors to track targets with sufficient accuracy before an ABI can be launched. Initial target tracking is done while the missile passes through the “afterburning” region. The time it takes to develop an accurate track depends on the resolution of the sensor, its frame rate, and the trajectory of the ballistic missile as viewed by the space-based infrared sensor. In particular, the target heading must be known with sufficient accuracy to know that the missile is on a threatening azimuth and so the KKV can remove residual errors in the predicted intercept point. In general, the more fuel a KKV carries, the larger the heading errors it can accommodate. However, adding fuel to compensate for large heading errors is not an attractive approach because of the increased KKV weight.

Different criteria can be postulated for target tracking. This analysis assumes that the target must appear threatening, that is, heading toward territory to be defended, and that the target heading must be known well enough so as not to impact seriously the KKV divert fuel requirement. To appear threatening, it is assumed the target missile must travel a minimum of two pixels (2–3 km from the original point of detection for a 1 km × 1 km pixel footprint) to determine the approximate target heading before ABI launch, that is, the target heading must be determined to within approximately ±15 degrees.<sup>9</sup> This time is longer for lofted trajectories because the horizontal component of the missile’s velocity is lower.

In addition, this analysis assumes that the ABI launch would be further delayed if the track heading is not known well enough so that *after* the ABI booster burns out (i.e., 20 sec after ABI launch), the KKV has to expend more than 10 percent (i.e., 0.2 km/sec) of its divert budget to compensate for residual heading errors.<sup>10</sup> This leaves the majority of the KKV fuel to compensate for target maneuvers during its boost phase, which drives the KKV divert budget. The lateral divert required to correct for initial heading errors can be provided by the ABI rocket motor during its boost phase using in-flight target updates at little expense in ABI speed.<sup>11</sup> For the missile trajectories examined in this study, the 2-pixel requirement always dominated, that is, delaying the ABI launch until the target had traveled two pixels down range always resulted in less than 0.2 km/sec of KKV divert to correct for residual heading errors after the 20-second ABI boost phase ends.

The time delays shown in Table 1 are based on lofted North Korean and Iranian missile trajectories because they exhibit the longest track delays.<sup>12</sup> Depressed and minimum energy trajectories have longer target detection



delays because it takes longer to reach an altitude of 7 km along these trajectories, however, their tracking delays are shorter because the horizontal component of velocity is higher, which compensates for the detection delay thereby allowing the ABI to be launched several seconds sooner.

In some cases the time to track is shorter than five seconds. This analysis assumes that five seconds is a lower bound on the time to track for any sensor because several seconds will be needed for command and control decisions by local commanders (insufficient time exists to request launch authorization from higher authorities) and for communication delays between the sensor platform and the ABI launch platform.

The Scud B and the 180-second solid-propellant ICBM are the two target missiles with the most stressing timelines of the missiles examined in this study. A space-based infrared sensor with 1 km pixel dimensions should suffice to produce tracking times close to the minimum value for a 180-second burn time ICBM (see Table 1). However, faster tracking times for the Scud B missile would require higher resolution sensors. Sensor resolution would have to be reduced to approximately 0.5 km pixel footprints to ensure that most of the missiles examined in this study could be tracked within less than 5 seconds by a space-based infrared sensor. Whether the increased cost, narrower field of view, and longer scan times associated with such a sensor are acceptable can be determined only by conducting an overall system tradeoff study, which is beyond the scope of this analysis.

Note that booster typing would be very difficult soon after launch detection because staging events will not have occurred yet and the target's acceleration profile cannot be determined with sufficient accuracy from crude track data to determine the missile type, despite the fact that solid-propellant ICBMs have shorter tracking times than liquid-propellant missiles. Even with accurate acceleration profiles, as might be provided by radar or LIDAR, booster typing is challenging because medium-range ballistic missiles (MRBMs) and ICBMs can have similar acceleration profiles early in their boost phase, as indicated in Figures A4 and A5. Optical signatures might be exploited, but they may not be sufficiently distinct to discriminate booster types. Optical signatures might provide some information on whether the missile burns liquid or solid fuel—a factor that determines the approximate burn time—but this information too may be unreliable at the time of ABI launch. Consequently, one would be committing an ABI against a target with a bright plume without much knowledge of whether the target is a liquid- or solid-propellant, medium-range or intercontinental-range ballistic missile.

The final burnout points for theater-range and intercontinental-range ballistic missiles can vary by several hundred kilometers. Therefore, if one doesn't know the booster type, several ABIs may have to be launched to guard against

mistaking a theater-range missile for an ICBM and vice versa. In addition, ballistic missile boosters can maneuver in flight, for example, involving lofted or depressed trajectory maneuvers, plane changes, general energy management maneuvers (used by solid-propellant ballistic missiles to adjust their range), or intentional booster maneuvers to avoid intercept. Such maneuver can change the predicted intercept point by several hundred kilometers for ICBM targets even if the missile type is known and, hence, drive the KKV divert requirement because they must be compensated for entirely by the kill vehicle after the ABI booster burns out.<sup>13</sup> If missile boosters do not maneuver but rather fly along predictable trajectories, with sensor noise as the dominant source of trajectory error, then the predicted intercept point can be estimated to within a few kilometers or perhaps tens of kilometers, for most ballistic missiles shortly after the target is detected.<sup>14</sup>

The total ABI launch delay and the time remaining for ABI flight is also shown in Table 1. The total launch delay is simply the sum of the detection and tracking time delays. The ABI flight time is equal to the target missile boost time, minus the launch delay, minus the time before booster burnout that intercept should be achieved. Ballistic missile boost times can vary by up to 5 percent from their nominal values due to pressure and thermal effects that alter the fuel flow rate for liquid-propellant motors and the burn rate for solid-propellant grains. Thus, to be confident that an ABI can intercept its target before the rocket motor burns out, the intercept time before burn out (TBBO) should be at least 5 percent of the target's nominal boost time. In addition, to ensure that the debris lands well short of the intended target, ballistic missiles should be intercepted about 5 seconds prior to their nominal burn time. This causes the debris to land at a range about 15%–25% less than the missile's intended range (see Figure A6). If North Korean or Iranian ICBMs are intercepted 5 seconds before burnout, the debris would land in northern Canada (see Figures A7 and A8), well away from populated areas in Canada and the United States (except for North Korean trajectories that pass over Alaska).

## **Radar Detection and Tracking**

Radar provides all-weather tracking and very accurate range measurements. Airborne radar, in particular, can provide early ballistic missile detection, if the radar is approximately 400 km or less from the missile launch site because, at this range, an airborne radar flying at 12 km (40,000 ft) altitude has line of sight to the ground. Targets beyond this range must climb high enough to be seen over the radar horizon. Land and sea-based radar are less attractive,

unless they are located very close to the launch site, because target missiles take too much time to rise above the radar horizon to provide timely detection. For example, it takes between 70–110 seconds for targets to become visible to surface-based radar at a range of 600 km, depending on the missile type, the missile's trajectory and the radar grazing angle. However, surface radar can provide in-flight target update information to guide the KKV in flight. If effective radar jammers are deployed that eliminate radar range information, then the defense would have to deploy two or more radars to track targets using only angle measurements.

Radar can either use space-based infrared detection to cue the radar, thus avoiding a large search solid angle, or they can operate in stand-alone mode where the radar conducts a wide-area search along a section of the horizon to obtain initial detection. Clearly, if a radar is cued from a space-based infrared sensor, radar detection would occur after infrared detection. Since flight time is of the essence for boost-phase intercept, this analysis examines the potential for airborne radar to provide earlier detection times, thereby reducing the ABI launch delay and increasing the ABI flight time. Hence, the radars examined here are designed to operate in wide-area surveillance mode.

Airborne radar use range gates and Doppler processing to sort clutter returns from vehicle traffic and Doppler shifted returns from the earth's surface. This analysis assumes that a target's radial (Doppler) speed must exceed 150 km/hr before detection can occur. As a consequence, targets go undetected until their Doppler speed exceeds this value and target tracks are dropped when the target trajectory is nearly perpendicular to the radar line of sight. Target missiles launched at ranges closer than the radar horizon can be detected as soon as their Doppler signal exceeds 150 km/hr. However, accurate tracking typically cannot occur until the target is about half the radar elevation beam width above the horizon, as discussed below.

The airborne radar detection times listed in Table 1 have been computed by considering a range of launch locations throughout North Korea and Iran for different missile types, then selecting the worst-case time delay associated with the radar that is in the most favorable location for observing the target. This usually was an airborne radar near the DMZ for North Korean launches and varied for launches from Iran. In general, depressed trajectories have detection times several seconds longer than those listed in Table 1, depending on the exact launch profile for the first stage rocket motor (which may not be much different for depressed and lofted trajectories). However, lofted trajectories create worst-case intercept geometries because the higher intercept altitude decreases the ABI intercept range. Hence, the airborne radar detection times shown in Table 1 are for lofted trajectories.

The maximum radar detection range ( $R_{\max}$ ), for a radar operating in surveillance mode, is given by the radar range equation,

$$R_{\max}^4 = \frac{P_{ave} A_e \sigma \varepsilon_i(n) t_s}{4\pi k T_n (S/N)_1 L_s \Omega},$$

where  $P_{ave}$  is the average radiated power,  $A_e$  is the effective antenna aperture,  $\sigma$  is the target radar cross section,  $\varepsilon_i(n)$  is the efficiency with which the radar integrates  $n$  pulses,  $k$  is the Boltzmann constant ( $1.38 \times 10^{-23}$  J/deg),  $T_n$  is the radar antenna noise temperature,  $(S/N)_1$  is the signal-to-noise ratio required to detect the target with a specified probability and false alarm rate with one pulse,  $L_s$  includes various loss factors associated with the radar and the propagation path, and  $t_s$  is the time required to scan a solid angle  $\Omega$ .<sup>15</sup> Thus, in surveillance mode, radar capability is determined largely by the power-aperture product and the time required to scan one steradian in solid angle. The solid angle is determined by the azimuth to be scanned—assumed to be 90 degrees in this analysis—and the height of the scanned sector—assumed to be one beam height. The scan time per steradian is determined by  $n/(f_p \Omega_0)$ , where  $n$  is the number of pulses integrated for detection in surveillance mode,  $f_p$  is the radar pulse repetition frequency and  $\Omega_0$  is the solid angle of the radar main-lobe beam.

Liquid- and solid-propellant ICBMs are assumed to have a minimum radar cross section (i.e., nose-on) at 10 GHz of approximately 0.5 m<sup>2</sup> and 0.1 m<sup>2</sup>, respectively.<sup>16</sup> However, within a few tens of seconds after launch most missiles are 20–40 degrees from vertical and, hence, their radar cross sections will be larger. In addition, the aft radar cross section is larger than the nose-on cross section. Hence, if the missile flies away from the radar, as is the case with North Korean ICBM launches viewed by an airborne radar south of the DMZ, it will have a larger radar cross section. This analysis assumes a minimum radar cross section of 0.5 m<sup>2</sup> for initial launch detection. The radar cross section for tracking is lower, especially after staging events, and is assumed to be 0.1 m<sup>2</sup> and 0.5 m<sup>2</sup> for solid and liquid propellant ICBMs, respectively. To obtain reasonable tracking ranges, assumed here to be at least 650 km, additional radar pulses must be integrated.

Table 2 gives the parameters for several notional radars examined in this study. The ground-based radar (GBR) is similar in design to the THAAD Ground-Based Radar but with a power-aperture product about twice as large to obtain sufficient detection ranges and fast scan times. The sea-based radar (SBR) is similar to the Aegis SPY-1B radar with an increase in power-aperture product of about 70 percent. Finally, the notional airborne X-band radar (not

**Table 2:** Radar parameters and estimated performance<sup>a</sup>.

	Ground-based X-band radar	Sea-based S-band radar	Airborne X-band radar
<b>Parameter</b>			
Operating frequency (GHz)	9.5	3.3	10
Pulse repetition frequency <sup>b</sup> (Hz)	45	17	30
Total average power (kW)	120	100	120
Antenna height (m)	2.0	3.85	2.0
Antenna width (m)	4.6	3.65	4.0
Physical aperture (m <sup>2</sup> )	9.2	14.1	8.0
Effective aperture (m <sup>2</sup> )	6.0	12.0	5.2
Power-aperture product (kWm <sup>2</sup> )	720	1,200	624
Receiving gain (with weighting)	75,400	18,200	72,600
Weighted azimuth beam width (deg)	0.44	1.60	0.48
Weighted elevation beam width (deg)	1.01	1.52	0.96
Azimuth scan sector (deg)	90	90	90
Search solid angle (sr)	0.0278	0.0415	0.0264
Beam solid angle (sr)	1.36E-04	7.38E-04	1.41E-04
Noise temperature (°K)	500	500	650
System and atmospheric losses (dB)	19.5	18.4	19.2
<b>Performance<sup>c</sup></b>			
Time to transit elev. beam <sup>d</sup> (sec)	8.8	13.2	16.8
Surveillance scan time (sec)	4.5	6.6	6.2
Pulses integrated for surveillance	1	2	1
Surveillance range: 0.5 m <sup>2</sup> target (km)	585	730	590
Track integration time (sec)	0.33	0.53	0.50
Pulses integrated for tracking	15	9	15
Tracking range: $\sigma = 0.1/0.5$ m <sup>2</sup> (km)	650/970	650/970	655/980

<sup>a</sup>Many of these radar parameters come from the APS study, *Boost-Phase Intercept Systems for National Missile Defense*, July 2003, Sections 10.2.3–10.2.5.

<sup>b</sup>The estimated pulse repetition frequency assumes that only a few pulses are integrated in surveillance mode. In any case, the pulse repetition frequency cannot exceed 100 Hz to avoid range ambiguities for a maximum detection range of 1,500 km.

<sup>c</sup>The detection probability is assumed to be 0.90 with a false alarm probability of  $10^{-6}$ , requiring a single-pulse signal-to-noise level of 20.8 dB. The cumulative detection probability is 0.99 for two scans.

<sup>d</sup>The maximum elevation rate for missile targets crossing the GBR, SBR, and ABR elevation beams is 2 mrad/sec, 2 mrad/sec and 1 mrad/sec, respectively.

to be confused with the Airborne Warning And Control System, or AWACS, S-band radar used for air defense) is designed with sufficient power-aperture product to have long detection ranges and fast scan times. This airborne radar (ABR) is a conformal array and essentially has the performance of an airborne THAAD-like radar. X-band was chosen over S-band despite the increased difficulty in achieving high transmit power and greater atmospheric

attenuation, because the beam can scan closer to the horizon, thus detecting targets earlier.

The radars in Table 2 are designed to be powerful enough to scan 90 degrees in azimuth in half the time it takes a target booster to transit the radar elevation beam width, which for the missiles examined in this analysis is between 9 and 17 seconds.<sup>17</sup> Short scan times also minimize the scan delay for initial target detection, which arises because the radar may be scanning another part of its surveillance volume when the target first appears above the horizon. This delay is, on average, half the surveillance scan time. The radar power-aperture product is adjusted to obtain a probability of detection of 0.9 on each pass, resulting in a cumulative detection probability of 0.99. This requires a single-pulse signal-to-noise ratio of 20.8 dB for a false alarm rate of  $10^{-6}$ . The tracking range for each radar is designed to be approximately 650 km and 1,000 km against  $0.1 \text{ m}^2$  and  $0.5 \text{ m}^2$  targets, respectively, with a track integration time between one-third and one-half of a second.

Radar track accuracy depends on the radar frequency, the dimensions of the antenna, the radar signal-to-noise level, the degree to which the target radar cross section fluctuates, and propagation effects, especially when viewing targets close to the horizon. As a rule of thumb, angular track accuracies on the order of one-tenth of the diffraction-limited beam width ( $\theta_b$ ) can be achieved. Multipath effects are the dominant source of error for low-angle tracking (i.e., for targets within  $1.5 \theta_b$  of the horizon). These errors can be reduced by using narrow beam widths (i.e., high radar frequencies and tall antennas) and by sophisticated signal processing (e.g., high range resolution, frequency diversity, and off-axis tracking techniques). In general, low elevation angle track errors on the order of  $0.1 \theta_b$  can be obtained without too much effort for targets located at grazing angles at least  $0.3 \theta_b$  to  $0.5 \theta_b$  above the horizon.<sup>18</sup> This analysis assumes that the minimum grazing angle for accurate tracking is  $0.5 \theta_b$ . Therefore, the X-band radars in Table 2 can track targets with an angular accuracy of approximately 0.1 degrees, which translates into a position error of approximately 1 km at a range of 600 km.

The range resolution, on the other hand, for modern tracking radar can be on the order of a few meters, or less. Consequently, in a jamming-free environment, track accuracies on the order of tens of meters or better can be obtained in the horizontal plane if multiple radars track the target. Vertical accuracies would remain on the order of 1 km until the target climbs fairly high above the horizon. If effective radar jamming is assumed on the part of the opponent, the accuracy drops to approximately 1 km in all three dimensions. Therefore, in a jamming-free environment, the radars in Table 2 could develop a track accuracy enough to launch an airborne interceptor within five seconds after initial

radar detection, including several seconds for command, control and communication time delays, because the target heading error can be determined to within  $\pm 2$  degrees in two seconds. Two seconds is chosen because it is assumed that three out of four radar hits are required to establish a track. In a jamming environment the radar tracking delay would be comparable to that for a 1 km pixel space-based infrared sensor. Such rapid tracking may seem optimistic, however, it should be achievable if one designs the surveillance architecture with rapid target detection and tracking in mind. Note that this leaves very little time for human intervention in the ABI launch process—essentially a simple “go-no go” decision on the part of a tactical commander. This may seem risky, however, it is of less concern than one might think for a defensive system brought to a high state of alert in the midst of a crisis, as argued below.

Figure 2 illustrates various boost-phase trajectories associated with medium and long-range missiles launched from North Korea. The ICBM launch

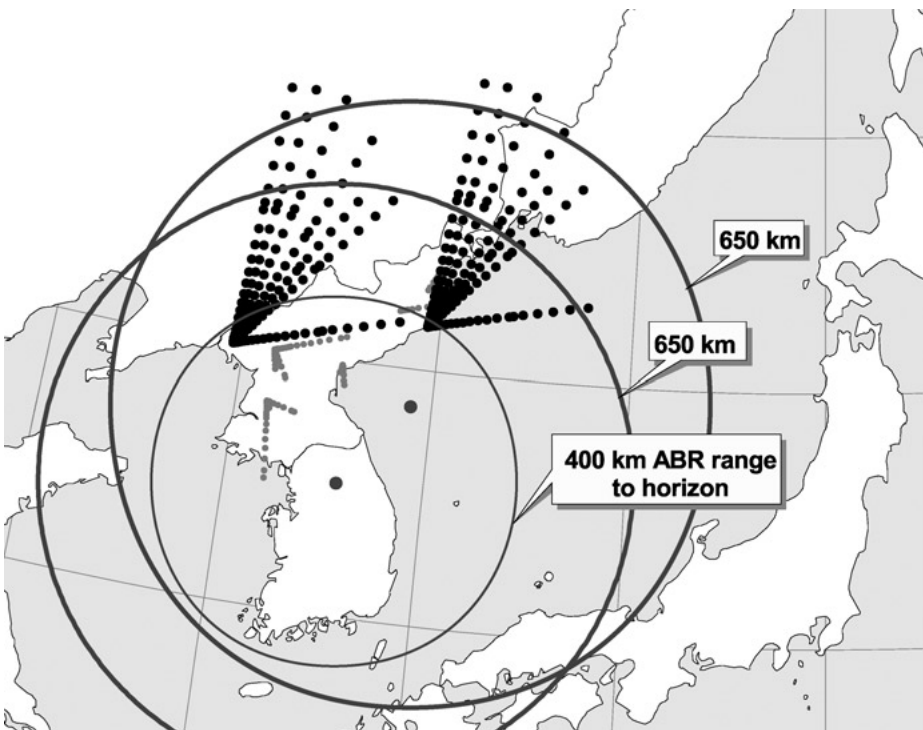


Figure 2: Sensor coverage.

fans correspond to a 240-second liquid-propellant ICBM heading toward targets spread across the United States from the east to the west coasts (including Alaska), with one outlying trajectory on the right-hand side heading toward Hawaii. Each dot represents the ground track of the booster at 10-second intervals. A 290-second liquid-propellant ICBM would have slightly longer boost-phase tracks and a 180-second solid-propellant ICBM would have shorter boost-phase tracks. The shorter boost-phase tracks (in gray) in Figure 2 represent Scud B, Scud C, No Dong and Taepo Dong missiles. The circles indicate the range from a radar location approximately 80 km south of the DMZ and another 120 km off the coast of North Korea in the Sea of Japan. As one can see, tracking ranges of 650 km are sufficient to support boost-phase intercept against North Korea because the KKV homes autonomously during the last 100 km of its flight (recall that the intercept occurs approximately 10–20 seconds before booster burnout, as indicated in Table 1).

Figure 3 illustrates the time it takes ground, naval, and airborne radars to detect ICBMs launched from the western-most launch location in North Korea (the worst-case) heading toward Chicago. The ground-based radar is assumed to be located near Vladivostok and the naval radar is collocated with the airborne radar in the Sea of Japan. An airborne S-band radar (ABR-S) with similar detection range and surveillance characteristics to the airborne X-band radar

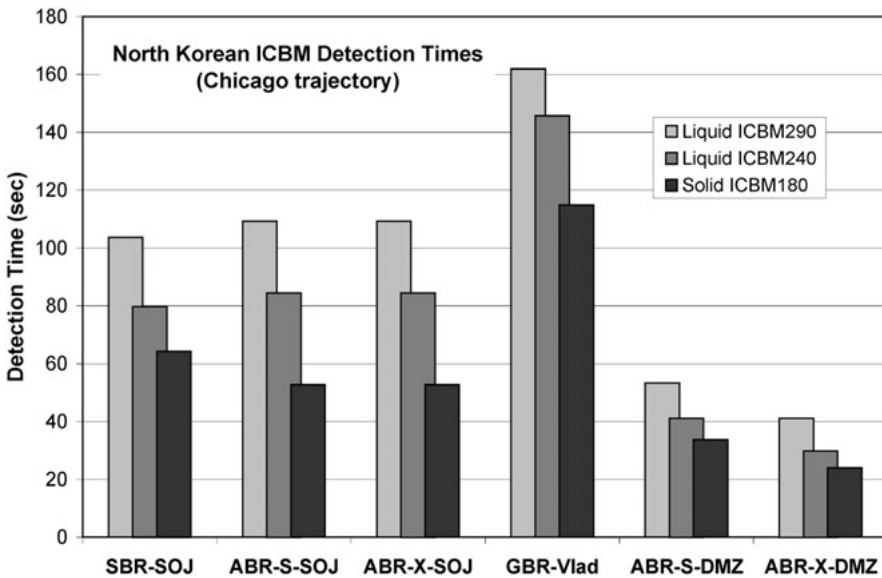


Figure 3: Radar detection times for North Korean ICBMs.



(ABR-X) in Table 2 is also shown to make the point that X-band radar can provide earlier detection times due to its lower grazing angle. Solid-propellant ICBMs are detected earlier than slower liquid-propellant ICBMs, as one might expect, because they enter the radar surveillance fan earlier and have higher Doppler speeds. The airborne radars near the DMZ clearly have the shortest detection times.<sup>19</sup> An airborne radar over the Sea of Japan has the same favorable viewing geometry but, for a trajectory heading toward Chicago, is limited by the Doppler notch because the trajectory is nearly perpendicular to the radar's line of sight early in the missile's flight.

Figure 4 illustrates a similar radar surveillance picture for Iran. Three or more radars must be present continuously to provide adequate coverage of hypothetical Iranian ICBM launches, especially if the radar has only a 90-degree azimuth search capability (the azimuth limitation is not illustrated in the figure). Medium-range ballistic missiles, as illustrated by the short boost-phase tracks (in gray) in Figure 4, require airborne radar flying along the Iraq-Iran border for adequate launch detection—clearly a difficult proposition. Although

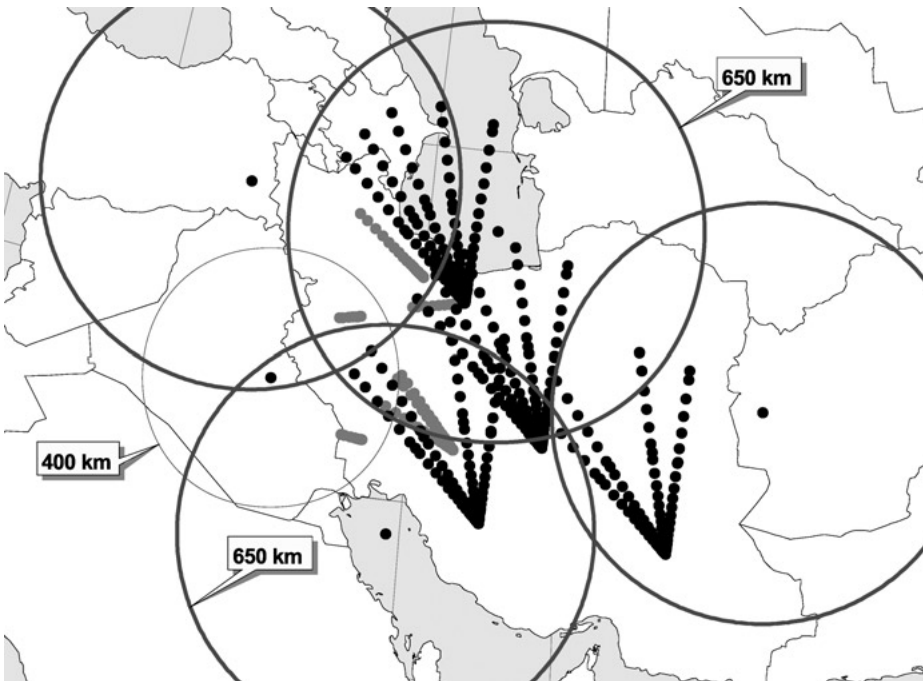


Figure 4: Radar coverage of Iran.

airborne radar appears to provide adequate coverage of Iran, this state is large enough that the radar detection ranges are beyond the horizon and, hence, slower (by about 15 seconds for ICBMs, as shown in Table 1) compared to similar radar detection times from North Korea. In fact, they are a bit longer than space-based infrared detection and tracking times. Consequently, space-based infrared systems provide the best sensor architecture for Iran. Airborne radar is an important adjunct to space-based detection and tracking over Iran, especially for theater-range missiles launched from sites around the periphery where the viewing geometry is more favorable, assuming airborne radars have access to adjacent airspace.

To summarize, space-based infrared sensors probably are the preferred sensors for boost-phase detection and tracking, particularly for large countries such as Iran. Sensors with 1 km footprints on the Earth's surface should be sufficient for boost-phase detection and tracking, although 0.5 km footprints might be attractive under some circumstances. Consequently, a sensor like SBIRS-High, assuming it has characteristics similar to the notional space-based infrared sensor examined here, should have high priority in any future boost-phase missile defense architecture. Airborne X-band radar can achieve more rapid detection and tracking in favorable geographies, thus leading to greater ABI intercept ranges against small states like North Korea. In addition, as a second detection phenomenology, it can reduce false alarms and make boost-phase decoys more difficult to construct when compared to a detection and tracking architecture that depends solely on space-based infrared sensors. However, airborne radars have limited endurance—approximately 8–12 hours on station, depending on the scenario—thus requiring three to four aircraft to keep one airborne 24 hours a day during a crisis. As a result, airborne radar is unattractive for continuous peacetime surveillance. Ground-based and sea-based radar can produce accurate target track data for in-flight target updates to the ABI, but the curvature of the earth limits their ability to detect targets soon after launch unless they are very close to the launch location.

## **KINETIC KILL VEHICLE DESIGN**

Kinetic kill vehicles for boost-phase missile defense involve greater technical challenges than KKV's for midcourse ballistic missile defense, such as the one currently undergoing flight tests as part of a thin US national missile defense system, because boost-phase KKV's must home on accelerating targets. This places greater demands on the homing guidance system, the amount of fuel required for homing, and the required peak KKV acceleration. In addition, the KKV initially must home on the rocket plume, then switch to home on

the missile body during the end game. For engagement geometries where the KKV sensors view the missile body through the plume, this can be a challenge. However, multispectral sensors and illumination of the missile body with an onboard LIDAR should meet this challenge.

Homing on the payload section of the target missile would be required if one is concerned about live warheads landing on another country's territory. KKV lethality against boosters should be high because accelerating missiles undergo large axial loads that cannot be carried if the missile structure is weakened by a projectile passing through the missile body and, perhaps, not even if the KKV passes through the payload section of the missile. Consequently, KKV impact will lead to the rapid collapse of the missile structure, resulting in a rapid reduction of the axial thrust, although some residual thrust may exist in random directions. If the payload section is intact, it will continue to fly on a ballistic trajectory, albeit at significantly reduced range. Various "lethality enhancement" techniques have been suggested to increase the chance that the payload and the booster will be destroyed in a single shot, but their effectiveness is not assessed here. Suffice it to say that boost-phase intercept still is effective, although politically less attractive, if it destroys the booster even if the warhead survives.

Boost-phase KKV's should be designed to be as light as possible because this proportionally reduces the mass of the interceptor missile, for a given interceptor speed. Airborne interceptors, in particular, should be as light as possible due to limited aircraft payloads, especially for fighters and unmanned aerial vehicles (UAVs). The upshot of this section is that boost-phase KKV's weighing 50–90 kg and having 2.0 km/sec divert capability are technically feasible using current technology. Advances in lightweight propellant tanks, divert rocket motors and sensor suits may allow 25 kg KKV's with 2.0 km/sec of divert capability to be built, although this would be challenging within the next decade. Claims that boost-phase KKV's can be built with a mass as low as 10 kg are quite optimistic, although such lightweight KKV's do not violate the laws of physics.

Exoatmospheric and endoatmospheric KKV designs are quite different because the aerodynamic drag and lift forces on KKV's operating below 40 km intercept altitude substantially affect their performance. Endoatmospheric KKV's require a shroud to reduce aerodynamic drag and a window to protect the infrared sensors from overheating. At ABI speeds above 4 km/sec, low altitude (25–30 km) intercepts become difficult due to aerodynamic window heating—heating levels reach 1,000 MW/m<sup>2</sup> at this speed and altitude, thereby requiring special window designs or active window cooling.<sup>20</sup> For this reason, Scud B intercepts, which occur at these altitudes, are challenging, in addition to their short boost time. However, endoatmospheric KKV's have an advantage in that

**Table 3:** Boost-phase kinetic kill vehicle designs.

Property	Baseline exo-KKV	Advanced exo-KKV	Baseline endo-KKV	Advanced endo-KKV
Mass breakdown				
Seeker mass (kg)	7.0	4.9	3.6	2.5
Avionics mass (kg)	9.5	6.7	9.3	6.5
Engine mass (kg)	11.4	5.8	10.3	5.5
Tank mass (kg)	10.9	3.8	4.5	1.8
Structural mass (kg)	3.5	2.5	9.5	5.6
Propellant mass (kg)	44.2	24.7	16.5	9.8
Total KKV mass (kg)	86.5	48.3	53.5	31.7
Other properties				
Total divert (km/sec)	2.0	2.0	1.0	1.0
Final KKV accel. (g)	15	15	15	15
Divert thrust (kN)	6.2	3.5	5.5	3.2
Divert isp (sec)	285	285	280	280
Propellant fraction	0.51	0.51	0.31	0.31

they can maneuver with aerodynamic lift forces, thus requiring less fuel for divert maneuvers. Exoatmospheric KKV, on the other hand, do not have to contend with atmospheric drag. But, in general, they have higher closing velocities with their targets and larger fuel loads because they maneuver entirely by divert propulsion.

To arrive at a plausible estimate for the mass of a boost-phase KKV, this analysis estimates the mass of different subsystems based on analogies with other systems. Table 3 illustrates the mass breakdown for the key subsystems: seeker, avionics, divert engines, propellant tanks, structural mass, and propellant. The exoatmospheric KKV, in this table have been designed to have a total divert capability of 2.0 km/sec and a final acceleration of 15 g in the homing end game. The seeker and avionics masses are based on analogy with the Clementine experiment, which used a KKV-like sensor to map the surface of the moon.<sup>21</sup> The structural mass for exoatmospheric KKV is assumed to be 3.5 kg, although lighter designs may be devised through clever use of the tanks for structural support.

The divert rocket engine mass is based upon the mass of four Rocketdyne LEAP KKV divert engines scaled to different thrust levels by the thrust-to-mass scaling ratio for satellite divert engines (a similar class of divert engines). Figure 5 shows the least-squares fit to satellite divert and attitude control engines along with three data points for the weight-to-thrust ratio of existing KKV divert engines.<sup>22</sup> Note that the satellite divert engines are heavier than the KKV divert engines because they are designed to survive in space for many years, undergo repeated firings, and potentially burn for a total of several hours

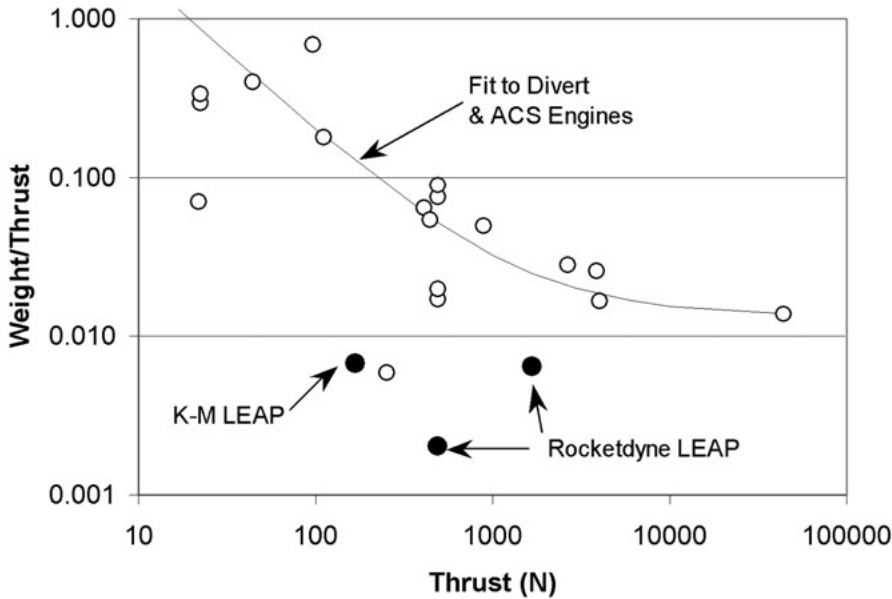


Figure 5: KKV divert engine scaling.

whereas KKV divert engines can be hermetically sealed until they are used once and they only burn for a total of a few minutes. Using the scaling relationship for satellite divert and attitude control engines and fitting it to four times the weight-to-thrust ratio of the heaviest Rocketdyne LEAP KKV engine with a thrust of 1668N (i.e., a cruciform arrangement of KKV engines), one obtains the following scaling relationship for the total KKV engine mass:

$$W_e = 0.0136T + 27,$$

where  $W_e$  is the weight of all four rocket engines (including the attitude control thrusters which are a small part of the total mass) in Newtons and  $T$  is the divert thrust of one engine in Newtons. This scaling relationship is appropriate for pressure fed, bipropellant divert engines, which in this analysis is assumed to burn mono-methyl hydrazine and  $N_2O_4$ . This equation provides a conservative estimate for the KKV engine mass. Fitting the curve to the Kaiser-Marquardt LEAP engine (with a thrust of 165N) would provide a more optimistic estimate (the constant term would be 4N instead of 27N), and fitting to the lighter 485N Rocketdyne LEAP engine would provide an even more optimistic scaling relationship.

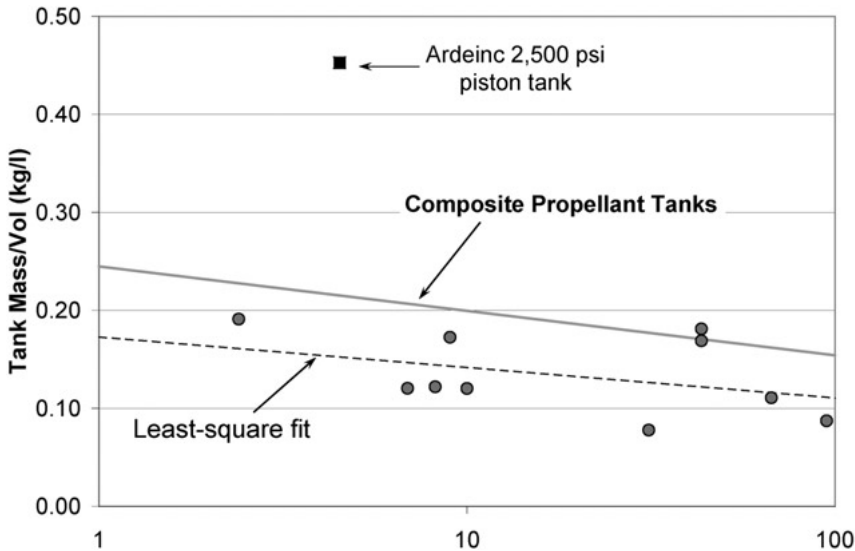


Figure 6: Propellant tank scaling relationship.

Propellant tank mass is calculated by scaling the tank dry mass to volume ratio for currently available composite propellant tanks, assuming the tanks operate at 2,500 psi, and that they are outfitted with a diaphragm to reduce propellant sloshing and to control the center of mass of the KKV as propellant is consumed. Diaphragms add approximately 40 percent to the tank dry mass.<sup>23</sup> High pressures are assumed because this increases the thrust for pressure fed liquid-propellant engines. Figure 6 illustrates a least-square fit (dashed line) to the mass-to-volume ratio for existing composite pressure tanks without diaphragms (the circles) rated at 2500 psi operating pressure.<sup>24,25</sup> Adding the mass of diaphragms, determined from existing lower pressure titanium propellant tanks commonly used on satellites, to the mass of composite pressure tanks, one arrives at an estimate for the mass of composite propellant tanks as shown in Figure 6 (solid line).<sup>26</sup> For comparison, an existing Ardeinc propellant tank with a piston, as opposed to a lighter diaphragm, is also shown in the figure.<sup>27</sup> The resulting scaling relationship for 2500 psi composite propellant tanks with diaphragms is

$$M_t = V_t(0.245 - 0.0454 \log_{10} V_t),$$

where  $M_t$  is the tank dry mass in kilograms and  $V_t$  is the tank volume in liters. The propellant mass and, hence, volume are derived from the total KKV divert requirement discussed next.

An advanced technology version of an exoatmospheric boost-phase KKV is also shown in Table 3. It represents the mass that probably can be achieved within the next decade due to technical advances. This variant assumes a 30 percent weight reduction for the avionics and seeker masses due to advances in lightweight batteries, guidance computers, focal plane arrays, and optics. In addition, lightweight pump-fed engines are assumed with a corresponding drop in tank mass due to their lower operating pressure.<sup>28</sup> The weight of pump-fed bipropellant engines is assumed to be

$$W_e = 0.0136T + 10,$$

where  $W_e$  is the weight of four divert engines, including attitude control engines, in Newtons and  $T$  is the divert thrust of one engine in Newtons. The propellant tank dry mass is given by

$$M_t = V_t(0.128 - 0.0357 \log_{10} V_t),$$

where  $M_t$  is the tank dry mass in kilograms and  $V_t$  is the tank volume in liters for Titanium tanks (Aluminum would be lighter) rated at 250 psi operating pressure including diaphragms. The structural mass also has been reduced by 30 percent for the advanced KKV design. Other researchers have proposed lighter kill vehicles; in particular, Lawrence Livermore National Laboratory has designed a lighter advanced technology kill vehicle with better performance—a total divert capability of 2.5 km/sec—with a total mass estimated at 30 kg.<sup>29</sup>

The baseline endoatmospheric KKV used in this analysis is assumed to have a total divert capability of 1.0 km/sec because it uses aerodynamic lift for much of its maneuvering. Consequently, it requires less propellant. The final end game KKV acceleration still is assumed to be 15 g. The avionics mass is assumed to be nearly the same as the exoatmospheric KKV (the battery is a bit lighter), and the sensor suite is lighter due to the lack of a long-wave infrared sensor (which is ineffective for low-altitude intercepts due to window heating) and its associated cryogenic unit. However, the structural mass is considerably heavier due to the need for a shroud to reduce drag and to protect the KKV within the atmosphere. The shroud mass is assumed to scale as the square-root of the total KKV mass because this approximates how the strength of structural support elements vary with the force they must withstand. The structural masses for the endoatmospheric KKV's given in Table 3 are consistent with those of other, more detailed, studies.<sup>30</sup> The engine specific impulse (Isp) is a bit lower than for exoatmospheric KKV's to reflect endoatmospheric operation,

with no thrust enhancement assumed due to the interaction between the rocket exhaust and the air stream flowing past the KKV. This enhancement can be as large as 30 percent.<sup>31</sup> The advanced endoatmospheric KKV is assumed to have 30 percent lower avionics and seeker masses, pump-fed divert thrusters, a lighter tank mass, and a reduced structural mass.

The KKV divert capability required to home on a target can be determined from the appropriate guidance law for homing guidance systems. The propellant mass required to achieve this divert can be calculated from the rocket equation. The divert required to compensate for a given miss distance can be calculated using proportional navigation guidance laws and the divert required to home on a target undergoing constant acceleration can be calculated using augmented proportional navigation laws.<sup>32</sup> However, neither proportional, nor augmented proportional, navigation is optimal for boost-phase intercept because booster acceleration is not constant.

More importantly, ballistic missiles can maneuver during their boost phase, thus introducing errors in the predicted intercept point that are quite large—on the order of several hundred kilometers between the predicted intercept point at the time of ABI launch and at the time of intercept for ICBM targets. As noted before, boost-phase maneuvers can occur whenever missiles are launched against targets whose range is less than the missile's maximum range. The excess propellant can be used to loft or depress the missile's trajectory, to carry out plane changes, or, in the case of some solid-propellant missiles, to implement general energy management maneuvers to reduce the missile's range.

Acceleration matching has been suggested as a better guidance law for boost-phase intercept in the recent APS Study and researchers at Lawrence Livermore National Laboratory have suggested a guidance law that optimizes both the time to go before intercept (i.e., the axial acceleration of the KKV) and the lateral divert requirement (i.e., the perpendicular acceleration) for boost-phase engagements.<sup>33</sup> The results of the APS analysis suggest that exoatmospheric KKV's will require 2.0–2.5 km/sec total divert capability to home on maneuvering ICBMs, including the effects of sensor noise, guidance time delays and different closing speeds between the KKV and its target.<sup>34</sup>

Figure 7 shows the results of a simple calculation that confirms the APS result. Here the total divert is calculated assuming the KKV matches the perpendicular component of the target's actual acceleration relative to what would be expected if the target did not maneuver during the boost phase. The engagement geometry is assumed to be one that maximizes the normal component of acceleration as viewed by the KKV (i.e., a worst-case). The divert requirements in Figure 7 represent averages between cases where the perpendicular



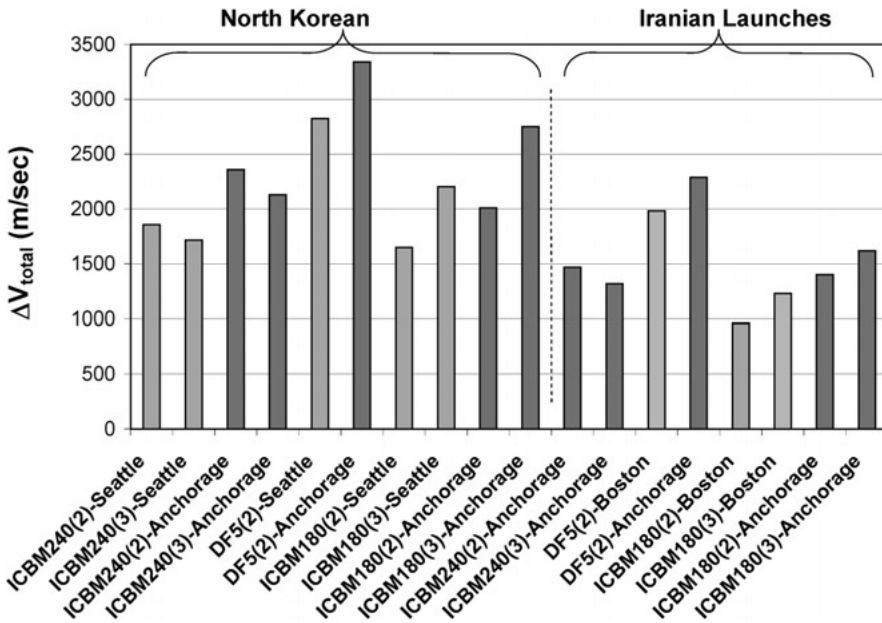


Figure 7: Divert requirements for different boost-phase intercepts.

component of the target acceleration arises from lofting or depressing the trajectory, where either the second or third stage (the stage is given in parentheses) is used to loft or depress the trajectory. The divert required to compensate for sensor noise (approximately 150 m/sec), end game homing (approximately 120 m/sec), and initial heading errors (at most 200 m/sec) are also included in the graphs shown in Figure 7.<sup>35</sup>

Figure 7 indicates that the required divert varies for different ICBMs launched against different cities in the United States. Note that missiles aimed at Anchorage, Alaska (the darker bars), from North Korea have more excess propellant than missiles aimed at Seattle (the lighter bars) and, hence, require greater KKV divert capability to intercept.<sup>36</sup> Similarly, if one assumes emerging states can build missiles as large as the Chinese DF-5 ICBM, or that the defense should be designed to be effective against large Russian or Chinese ICBMs, and that such missiles carry only one light warhead, thereby freeing up considerable fuel for maneuvers, then KKV's will require significantly greater divert capability (3.0–3.5 km/sec) for successful intercept. Finally, Iranian ICBMs require less divert to intercept than North Korean ICBMs, for identical missiles,

because they have less excess fuel for maneuvering (i.e., Iran is farther from U.S. territory and Iranian ICBM trajectories benefit less from the earth's rotation).

Therefore, one potential countermeasure to boost-phase intercept is to launch large liquid-propellant ICBMs toward targets at short range with small payloads, thereby maximizing the maneuver capability of the ICBM booster. The obvious counter-countermeasure is to build larger KKV's with more divert capability. However, these KKV's may be too heavy, depending on progress toward lightweight KKV designs, for airborne interceptors, thereby effectively ruling out an ABI option. Another possible countermeasure would be to launch ballistic missiles only on trajectories that require high KKV divert to intercept, thereby maximizing the chance that the KKV will run out of fuel. This is possible if the attacker knows the interceptor launch location, which would be the case for fixed ground-based launchers but not for airborne or naval launch platforms. Clearly, KKV's must either be designed with sufficient divert capability or their launch location must be unknown to the offense to render this tactic impotent.

Figure 8 illustrates the total KKV mass as a function of the total divert required for intercept. Exoatmospheric KKV's are illustrated in the left-hand graph and endoatmospheric KKV's in the right-hand graph. Clearly, the divert requirement has a strong impact on total KKV mass because not only is more propellant required, but the propellant tanks are larger, the divert engine thrust and, hence, mass is larger to achieve the same 15 g endgame acceleration, and the structural mass increases, all of which adds to the KKV dry mass.

In summary, exoatmospheric KKV's with a mass of approximately 90 kg and a total divert velocity of 2.0 km/sec should be technically feasible and should have the capability to intercept most emerging ICBM and intermediate-range ballistic missile (IRBM) threats. Similarly, endoatmospheric KKV's with a total divert velocity of 1.0 km/sec can probably be built with a mass of approximately 55 kg. Clearly, there is a premium on making the dry mass of the KKV as light as possible. More advanced KKV designs should be technically feasible within the next decade that can reduce this mass by 40–50 percent. Finally, to illustrate a more optimistic assessment, the Lawrence Livermore National Laboratory design goal for its exoatmospheric Advanced Technology Kill Vehicle for boost-phase intercept is shown in the left-hand graph in Figure 8—a design goal supported by considerable design experience even if a KKV with these characteristics has yet to be flight tested. Note that among the technical challenges will be the design of small, high-thrust divert engines because the required thrusts in Figure 8 are higher than that which has been achieved to date (see Figure 5).

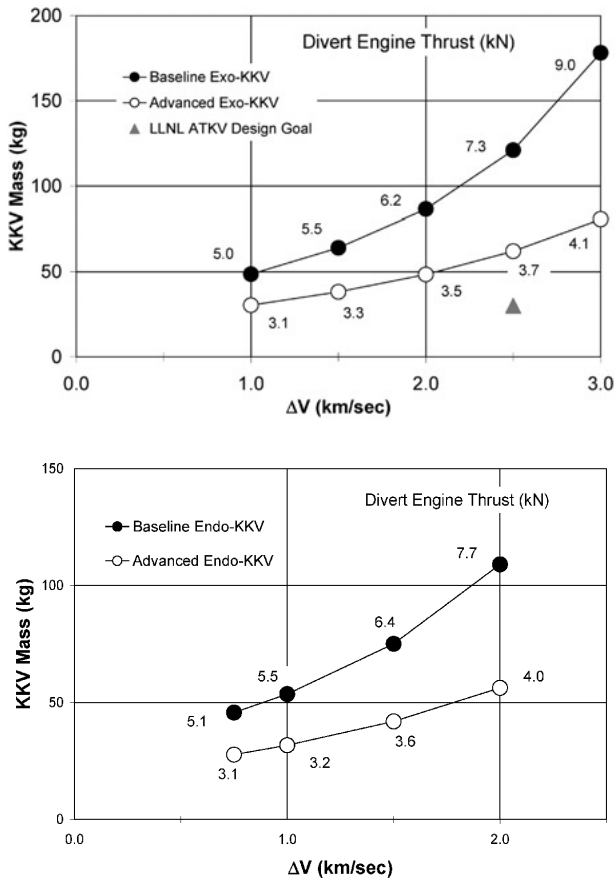


Figure 8: Exo- and endo-KKV mass versus divert requirement.

## AIRBORNE INTERCEPTORS

The ABI concept is based on a high-speed air-launched rocket with a KKV as its payload. ABI concepts originally were proposed in the early 1990s for theater missile defense, with fighter aircraft for launch platforms. Bombers and unmanned aerial vehicles (UAVs) have also been proposed, depending on ABI size and mass. In the early 1990s, the Raptor/Talon UAV-based ABI concept was designed for theater and national missile defense, with the emphasis shifting toward the larger Global Hawk UAV by the mid-1990s. The larger payload (1,000 kg), higher operating ceiling (60,000 ft) and longer endurance (24 hours)

of the Global Hawk made it an attractive launch platform for lightweight ABIs. Finally, a joint US–Israeli UAV-based ABI concept was pursued for theater missile defense in the mid-1990s, using the small Moab interceptor carried aboard an Israeli UAV. However, this program was cancelled in 1999. There is no active ABI program at the current time.

To achieve reasonable intercept ranges, ABIs should have flyout speeds of approximately 4–6 km/sec. These speeds require two-stage missiles. At speeds below 3 km/sec single-stage missiles are appropriate. The largest missiles that can be carried conveniently on rotary launchers or external pylons on existing U.S. heavy bombers would weigh approximately 1,500 kg.<sup>37</sup> For deployment on fighter aircraft, ABI masses should be less than about 1,000 kg. UAV deployment would require ABIs with masses of a few hundred kilograms each. Clearly, the lighter the ABI, the more that can be carried aboard any given launch platform.

Table 4 illustrates several optimally-staged ABI designs used in this analysis, with different ABI and KKV combinations. Any missile design involves complex tradeoffs between missile propulsion, structural design, and aerodynamic performance. Moreover, airborne missiles must be designed for

**Table 4:** Airborne interceptor designs.

Property	Baseline exo-KKV	Advanced exo-KKV	Baseline endo-KKV	Advanced endo-KKV
Total ABI mass (kg)	1,500	1,500	1,000	1,000
Ideal velocity (km/sec)	5.4	6.1	5.4	6.0
ABI length (m)	5.5	5.6	4.4	4.4
Maximum acceleration (g)	56	67	56	66
Total burn time (sec)	20	20	20	20
<b>Payload</b>				
KKV mass (kg)	86.5	48.3	53.5	31.7
Shroud mass (kg)	8.1	9.2	8.1	9.0
<b>Second Stage</b>				
Stage mass (kg)	232	197	154	134
Propellant mass fraction	0.81	0.81	0.81	0.81
Isp (sec)	280	280	280	280
Stage $\Delta V$ (km/sec)	2.35	2.7	2.4	2.7
Thrust (kN)	52	44	34	30
Stage burn time (sec)	10	10	10	10
<b>First Stage</b>				
Stage mass (kg)	1173	1245	785	825
Propellant mass fraction	0.85	0.85	0.85	0.85
Isp (sec)	280	280	280	280
Stage $\Delta V$ (km/sec)	3.0	3.4	3.0	3.3
Thrust (kN)	274	291	183	193
Stage burn time (sec)	10	10	10	10

extreme environments, in particular, thermal cycling, low temperature operation, and possibly high accelerations due to aircraft maneuvering. On the other hand, airborne missiles can be designed to accelerate faster than missiles launched from the surface of the earth due to the reduced drag force at high altitudes.<sup>38</sup> The ABIs listed in Table 4 have been modeled after existing air-to-air missile and ABI designs.<sup>39</sup> The ABIs with exoatmospheric KKV's have been designed to fit on heavy bombers, while the ABIs with endoatmospheric KKV's have been designed for deployment on fighter aircraft. The ABI shroud mass is calculated by scaling from a known missile shroud mass according to the square root of the maximum dynamic pressure the ABI experiences during flyout. The ABI propellant mass fractions are lower than one finds for typical ballistic missiles because more structural mass is required to handle the high axial accelerations during the interceptor's boost phase and the added mass of external fins for aerodynamic maneuver. The rocket motor specific impulse (Isp) is representative of modern solid-propellant rocket motors and the burn time has been selected to be short (20 seconds) to improve the intercept range for short flight times, although this increases the atmospheric drag at low altitudes. The actual flyout speeds for these missiles are approximately 0.5–1.0 km/sec less than the ideal velocity due to atmospheric drag and gravity, depending on the exact flight trajectory.

Lighter ABIs than the ones given in Table 4 can be designed with the same speed if the KKV mass is reduced, as illustrated in the left-hand graph in Figure 9 for a 5.4 km/sec ideal velocity. For example, a KKV would have to weigh approximately 30 kg for a 5.4 km/sec ABI to weigh 500 kg, that is, a mass that allows several to be carried on a high-altitude UAV and about 8 to 12 to be carried on a single fighter aircraft. Similarly, if the KKV mass is held constant, smaller ABIs give rise to lower ideal velocities, as illustrated in the right-hand graph in Figure 9 for 87 kg and 48 kg KKV's. For example, these KKV's would have 3.5 km/sec and 4.5 km/sec ideal flyout speeds, respectively, if the ABI mass is reduced to 500 kg. The 250 kg ABI masses in the right-hand graph in Figure 9 represent single-stage missiles.

## ABI INTERCEPT RANGES

The maximum ABI intercept range depends on the ABI speed and time; the latter of which depends on the target boost time, the time delay between ballistic missile and ABI launch, and the time before booster burnout required to ensure that the target debris falls well short of its intended target even for missiles whose burn times vary by 5 percent from their nominal burn times.

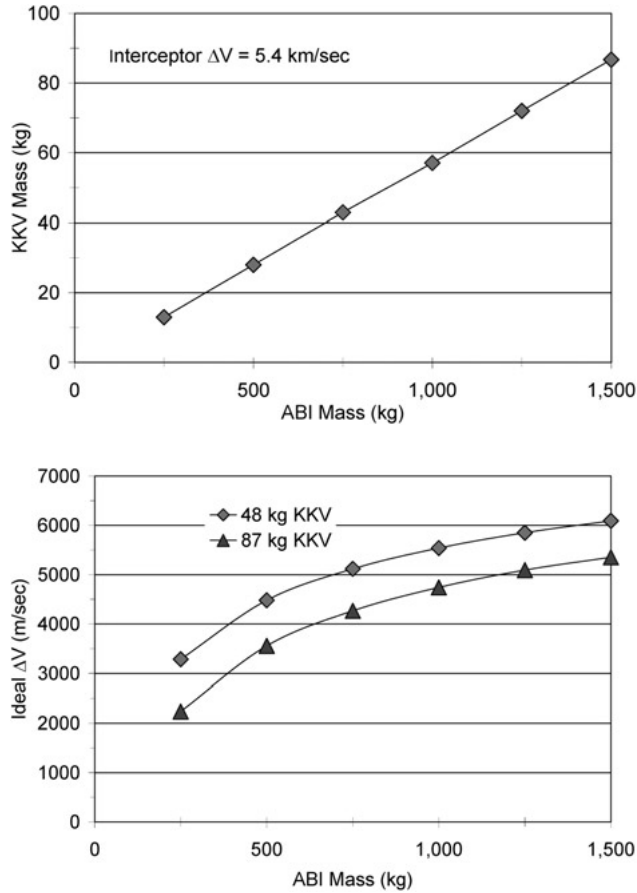


**Figure 9:** Capability of lighter ABIs.

A two-stage ABI based on current rocket-motor technology should be able to achieve speeds of approximately 4.5–5.0 km/sec (ideal velocities between 5.0–6.0 km/sec) with an 87 kg KKV as its payload, as discussed above. Boost times for theater-range ballistic missiles are typically between 60 and 150 seconds, depending on their range and design, whereas solid-propellant ICBM burn times are approximately 180 seconds, and liquid-propellant ICBM burn times are approximately 240–300 seconds, as shown in Table A1. The time delay between ballistic missile and ABI launch varies between approximately 20 seconds and 75 seconds depending on the sensor architecture and the target missile, as shown in Table 1.

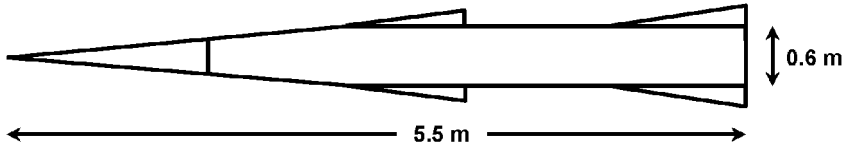


Figure 10: ABI hypersonic vehicle profile.

The intercept ranges for the ABIs in Table 4 are estimated by simulating ABI flight using the COMET code, modified to include atmospheric lift. This code takes into account the forces produced by the rocket propulsion system, gravity, inertial forces due to the earth's rotation, and the aerodynamic forces of lift and drag as the interceptor flies through the atmosphere.<sup>40</sup> Figure 10 illustrates a representative shape for the hypersonic ABIs listed in Table 4 (8 degree nose with a 2 cm rounded tip). The lift and drag coefficients for the vehicle shown in Figure 10 are illustrated in Figure 11, as a function of ABI speed and angle of attack. These coefficients were calculated using the Aero-Prediction Code AP02.<sup>41</sup> The lift and drag coefficients for the ABI second stage and the KKV are not shown, though they differ somewhat from those shown in Figure 10.

Figure 12 illustrates a flight fan for an exoatmospheric KKV launched from a 1,500 kg ABI, assuming the ABI follows a gravity turn after burnout. Such plots can be used to determine the approximate ABI intercept range by locating the ABI isotime contour that passes through the proper intercept altitude for a given target missile. However, in this analysis the ABI intercept range is determined using an optimal ABI flight profile where the ABI initially climbs higher in the atmosphere to minimize drag, then turns over to fly more horizontally to the intercept point. These optimal trajectories can increase the ABI intercept range by as much as 10 percent compared to those derived using Figure 12, though often the improvement is less than a few percent.

Table 5 gives the calculated intercept ranges using optimal ABI trajectories against a range of different North Korean and Iranian ballistic missile-trajectory combinations for the time delays associated with the space-based infrared sensors and airborne X-band radar given in Table 1. The ICBMs launched from North Korea are assumed to originate from the northwest corner of the country and those launched from Iran are assumed to come from the center of the country (near Yadz), thus providing worst-case intercept geometries for both countries (see Figures 2 and 4). All ballistic missile trajectories are lofted because this produces the shortest ABI intercept range, except for Scud B and

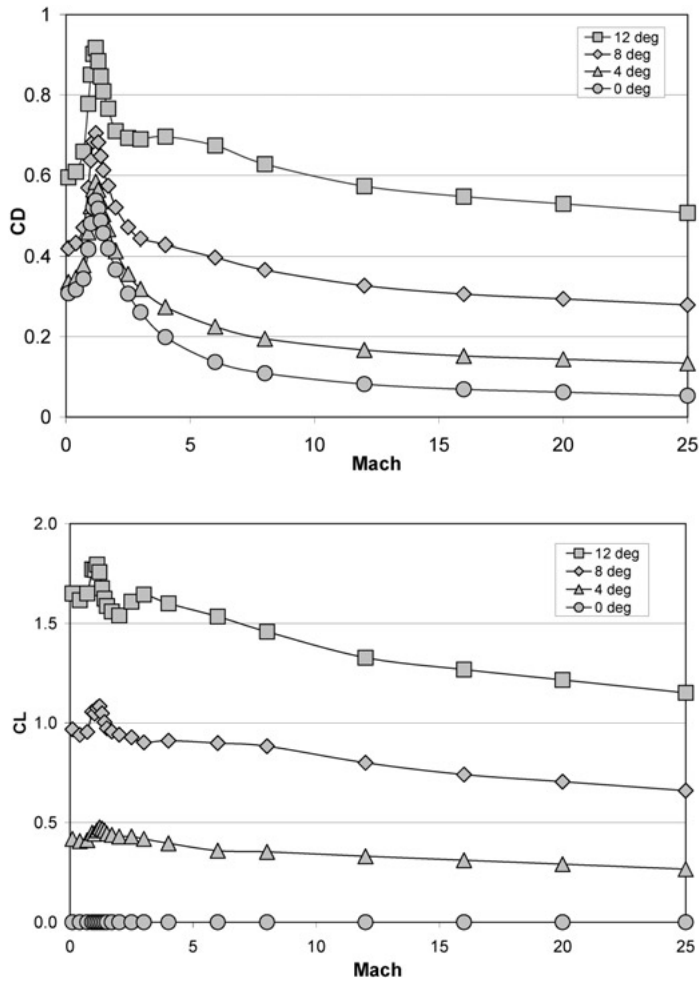


Figure 11: ABI lift and drag coefficients.

Scud C missiles, which are assumed to fly minimum energy trajectories. No Scud B or Scud C launches occur from Iran because these missiles do not have the range to threaten territory of interest to the United States. The Shahab 3, which is assumed to be identical to the No Dong, is the shortest-range Iranian missile examined in this study. The Shahab 4 is assumed to be identical to the Taepo Dong 1 and the Shahab 5 is a bit larger than the Taepo Dong 2 (see Table A1) to give it a range to strike most European capitals.



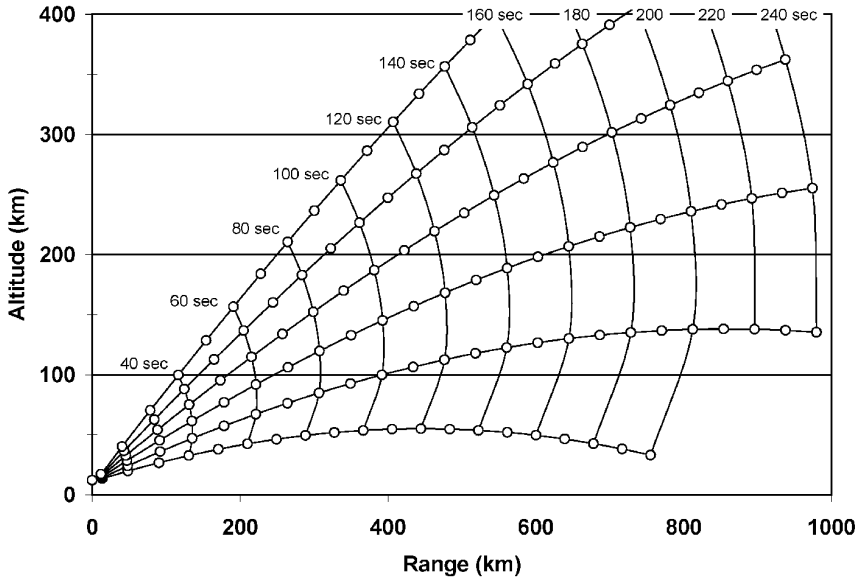


Figure 12: 1,500 kg ABI flyout fan.

Against North Korea, an airborne radar located approximately 100 km south of the DMZ usually detects the missile launches first. This location benefits from higher Doppler signatures because North Korean ICBMs fly away from the radar and MRBMs launched toward South Korea fly toward the radar. Airborne radars over the Caspian Sea or the Persian Gulf are the first to detect Iranian ICBM launches originating from central Iran. Iranian MRBMs launched from western Iran are first detected by whichever airborne X-band radar happens to be closest to the launch site. The average ground speed for North Korean ABI intercepts is approximately 4.2 km/sec and 4.8 km/sec for the baseline and advanced KKV designs, respectively, regardless of whether the intercepts are endoatmospheric or exoatmospheric, and the average ground speed for Iranian ABI intercepts is approximately 4.1 km/sec and 4.7 km/sec for the baseline and advanced KKV designs, respectively. Using these values, the reader can derive approximate intercept ranges for different flight times. Finally, launching ABIs from 60,000 ft instead of 40,000 ft reduces the atmospheric drag, thereby increasing the ABI range by approximately 10 percent compared to the values given in Table 5.

Several trends are apparent in Table 5. First, intercept ranges supported by space-based infrared detection and tracking sensors are about the same for

**Table 5:** ABI intercept ranges against North Korean and Iranian ballistic missiles.

ABI-target combinations	Intercept range (km)			
	1.0 km SBIRS		Airborne X-band radar	
	North Korea	Iran	North Korea	Iran
<b>1500 kg ABI—87 kg Exo KKV</b>				
290-sec ICBM-Boston	820	785	890	790
290-sec ICBM-Seattle	775	800	845	805
290-sec ICBM-Anchorage	745	775	820	780
240-sec ICBM-Boston	700	660	760	650
240-sec ICBM-Seattle	645	675	710	670
240-sec ICBM-Anchorage	605	640	670	630
180-sec ICBM-Boston	490	470	525	445
180-sec ICBM-Seattle	455	485	495	460
180-sec ICBM-Anchorage	425	460	470	435
Taepo Dong 1/Shahab 4	375	370	485	460
Taepo Dong 2/Shahab 5	490	495	580	510
<b>1500 kg ABI—48 kg Advanced Exo KKV</b>				
290-sec ICBM-Boston	935	905	1015	910
290-sec ICBM-Seattle	900	920	980	925
290-sec ICBM-Anchorage	880	900	960	905
240-sec ICBM-Boston	800	765	865	755
240-sec ICBM-Seattle	775	780	825	770
240-sec ICBM-Anchorage	730	750	795	740
180-sec ICBM-Boston	565	550	605	525
180-sec ICBM-Seattle	540	560	585	535
180-sec ICBM-Anchorage	515	545	565	515
Taepo Dong 1/Shahab 4	425	420	545	520
Taepo Dong 2/Shahab 5	560	575	660	590
<b>1000 kg ABI—54 kg Endo KKV</b>				
Scud B	0	—	105	—
Scud C	70	—	175	—
No Dong/Shahab 3	110	130	215	215
<b>1000 kg ABI—32 kg Advanced Endo KKV</b>				
Scud B	0	—	110	—
Scud C	80	—	185	—
No Dong/Shahab 3	125	145	235	235

North Korea and Iran, as one would expect. Second, the airborne X-band radar adds appreciably to ABI intercept ranges over North Korea since it can detect missiles soon after launch because the launch sites are within line of site of the radar, even when the radar is orbiting in protected airspace over South Korea or the Sea of Japan; whereas an airborne radar covering Iran would require access to neighboring airspace in Turkey, Turkmenistan, Afghanistan, and the Persian Gulf and, even then, has longer detection times because the target missile must climb above the radar horizon at a range of approximately 600 km for ICBMs launched from the center of Iran. In fact, a space-based infrared sensor with a 1 km pixel footprint yields longer ABI intercept ranges against Iranian

ICBMs than an airborne X-band radar. Therefore, space-based infrared sensors provide the best detection and tracking option for large countries like Iran with limited access to neighboring airspace. However, if airborne X-band radar can get close enough, longer intercept ranges can be obtained. Airborne radar has its greatest impact on boost-phase theater missile defense, as illustrated in Figure 13. Here, Scud B intercepts become feasible if the ABI platform flies over North Korean airspace and No Dong intercepts are possible from outside North Korean airspace.

Third, North Korean ICBM intercepts have approximately 10 percent shorter range against west coast trajectories compared to east coast trajectories because west coast trajectories have more excess fuel and, hence, higher lofted trajectories, thereby decreasing the ABI intercept range due to the fact that the ABI must climb higher in altitude (up to 400 km instead of 200–250 km) to intercept the missile. There is less variation in the ABI intercept range for different east and west coast Iranian ICBM trajectories because these targets are closer to the maximum range of the Iranian ICBM used in this analysis. Finally, intercepts against Iranian ICBMs heading for Seattle and Anchorage occur at longer ranges than the same missile-target pairing from North Korea because Iranian lofted trajectories burn out at lower altitudes and, hence, give rise to longer ABI intercept ranges, all other things being equal.

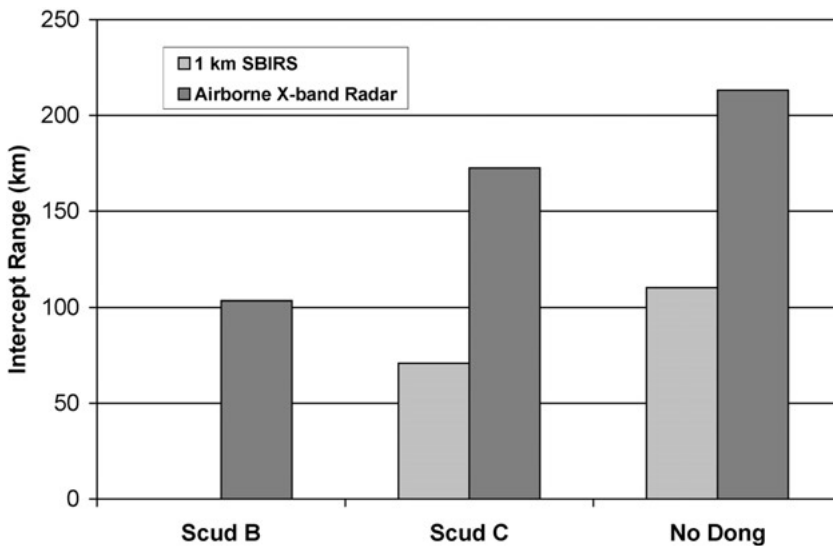
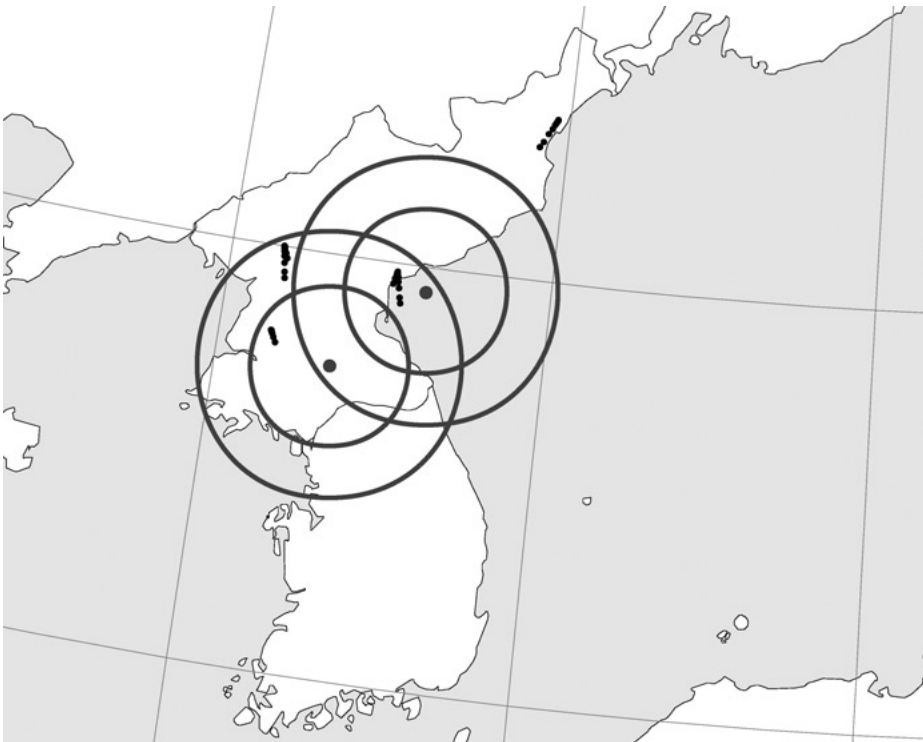


Figure 13: ABI intercept ranges for North Korean MRBMs.

ABI coverage is better illustrated using maps showing the worst-case ABI intercept ranges relative to the ground traces for different ballistic missile targets. For example, Figure 14 illustrates the intercept range against North Korean Scud B and Scud C missiles for a 1,000 kg ABI carrying the baseline endoatmospheric KKV and receiving launch detection and tracking information from an airborne X-band radar. The circles in the figure illustrate the ABI intercept range for an ABI platform located at the center of each circle. That is, any Scud B or Scud C missile that burns out within the respective circles is vulnerable to intercept by an ABI launched from the center of each circle.<sup>42</sup> The strings of dots in the figure represent the ground traces, shown every 10 seconds, for Scud B and Scud C boost phases. From Figure 14 one can surmise that it would take about three ABI orbits over or near North Korean airspace to cover all possible Scud B launches and about the same number to cover all possible Scud C launches (because they can originate from a larger



**Figure 14:** ABI intercepts against Scud B and Scud C missiles.

area due to their longer range). Fewer ABI launch locations would be required if potential ballistic missile launch locations can be identified using intelligence information. Note that an airborne X-band radar is essential to obtain such favorable coverage. Without the rapid target detection and tracking provided by such a radar, Scud B coverage disappears and Scud C coverage is reduced markedly (see Figure 13).

Figure 15 illustrates the hypothetical intercept range for 1,000 kg ABIs against No Dong missiles and 1,500 kg ABIs against Taepo Dong 1 missiles launched toward Japan, assuming space-based infrared detection and tracking with a 1 km pixel footprint. The longer ground traces are the Taepo Dong 1 boost phases. The thin outer circles in Figure 15 represent the No Dong intercept range using an airborne X-band radar. Consequently, No Dong launches can be intercepted using only two, or perhaps three, ABI launch locations outside North Korean airspace, but only if an airborne X-band radar is part of the sensor architecture. A single ABI site is all that is required to defend Japan and Okinawa from intermediate-range Taepo Dong 1 missiles, even with

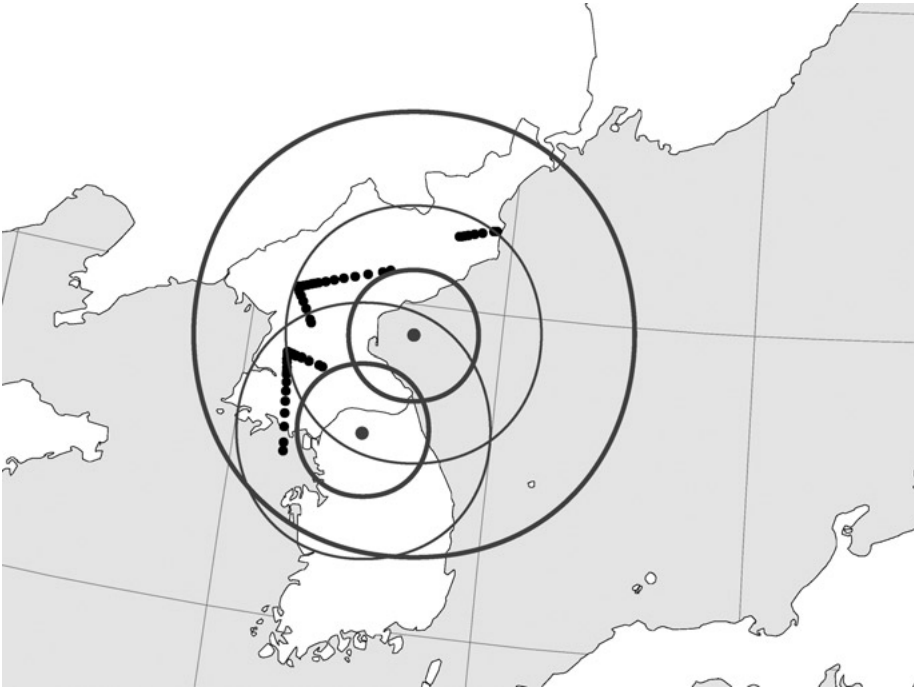


**Figure 15:** ABI intercepts against no Dong and Taepo Dong 1 missiles.

space-based infrared detection and tracking. Moreover, the latter ABI site could be far away from North Korean airspace over international waters in the Sea of Japan. Clearly, Taepo Dong 2 launches could also be intercepted from a single ABI launch location outside North Korean airspace.

Figures 16 and 17 illustrate similar plots for the intercept range associated with a 1,500 kg baseline exoatmospheric ABI launched from a location over the Sea of Japan approximately 100–150 km off the North Korean coast against hypothetical North Korean ICBMs with boost times of 240 and 180 seconds, respectively, assuming that space-based infrared sensors with 1 km pixel footprints detect and track the target. The ground traces for ICBMs launched towards the US east coast, west coast, and Hawaii (the lone eastward trajectory) are shown in the figures for two North Korean launch locations, providing an indication of the spread in azimuth for ICBM launches. The intercept ranges

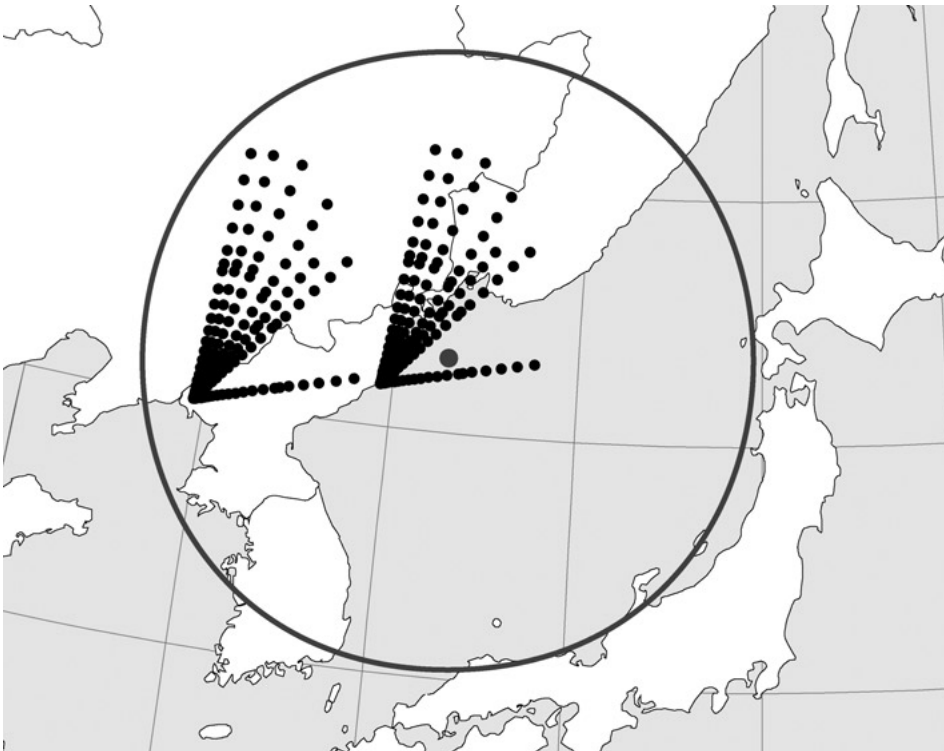


**Figure 16:** ABI intercepts against 240-sec liquid-propellant North Korean ICBMs.

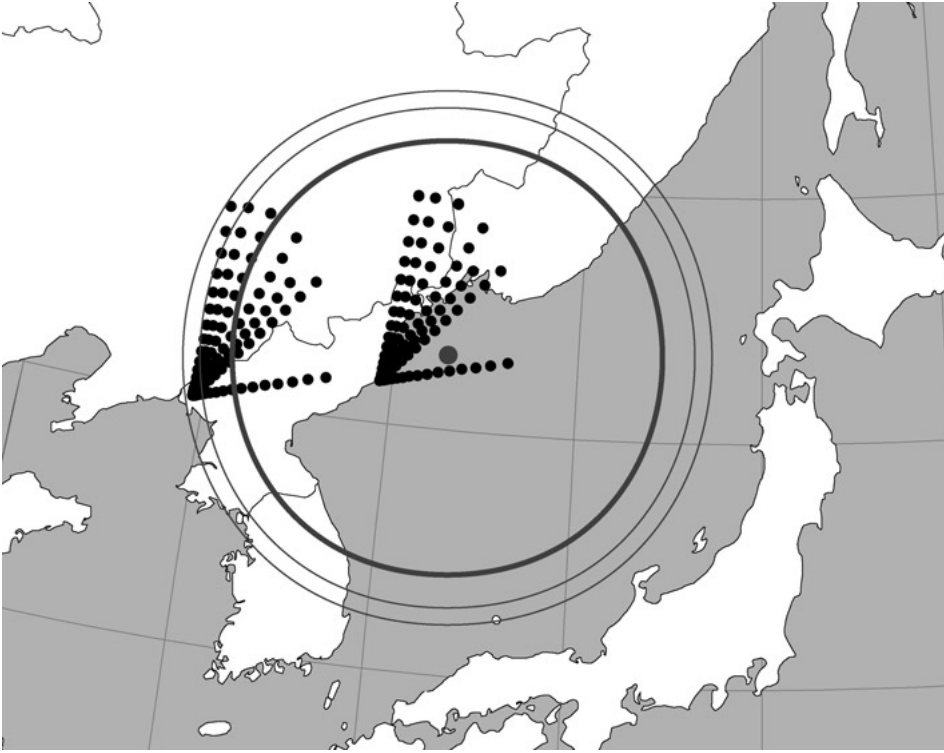


**Figure 17:** ABI intercepts against 180-sec solid-propellant North Korean ICBMs.

in Table 5 correspond to ICBM launches from the northwestern location. Obviously, North Korean ICBMs launched from the east coast of North Korea would be easier to intercept.

The two outer thin circles in Figure 17 correspond to improved ABI performance—the middle ring corresponds to an advanced exoatmospheric KKV using space-based infrared detection and tracking with 1 km pixel footprints and the outer ring corresponds to an advanced exoatmospheric KKV using airborne X-band radar for detection and tracking. Consequently, the 1,500 kg baseline exoatmospheric ABI using space-based infrared detection and tracking with 1 km pixel footprints should be able to intercept 240-second ICBMs, but not 180-second solid-propellant ICBMs. Clearly, ICBMs with burn times longer than 240 seconds also can be intercepted (e.g., the 290-second ICBM given in Table A1) because the added ABI flight time more than compensates for the longer range the ICBM can fly during its boost-phase.

The use of an airborne X-band radar improves the ABI intercept range and, when combined with a 48 kg advanced KKV, provides a capability to just intercept solid-propellant ICBMs, thereby providing a possible defensive response to this responsive offensive threat. Clearly solid-propellant ICBMs with burn times shorter than 180 seconds would be difficult to intercept unless the ABI has higher speed or flies closer to, if not over, North Korean airspace.

Figures 18 through 20 illustrate comparable ABI coverage against Iranian MRBMs and ICBMs. The ABI launch locations are approximately 100–120 km outside Iranian airspace. The range arcs for ABI intercepts are drawn assuming a space-based infrared sensor with 1 km pixel footprints for target detection and tracking. Higher resolution space-based infrared sensors would improve these intercept ranges somewhat. Airborne radar could also help, but only for missiles launched close to the periphery of Iran, that is, within approximately 400 km of the radar location.



**Figure 18:** ABI intercepts against Iranian Shahab-3, -4 and -5 MRBMs.





**Figure 19:** ABI intercepts against 240-sec liquid-propellant Iranian ICBMs.

The inner and outer circles in Figure 18 around the ABI launch locations over Turkey, the Caspian Sea and the Persian Gulf correspond to intercept ranges against Shahab 4 and Shahab 5 intermediate-range ballistic missiles, respectively, for a 1,500 kg ABI carrying a baseline exoatmospheric KKV and using space-based infrared sensors with 1 km pixel footprints. Consequently, the Shahab 5 can be intercepted from ABI launch locations outside Iranian airspace. However, the Shahab 4 could be difficult to intercept depending on its launch location. Shorter-range missiles like the Shahab 3 would be very difficult to intercept, even with a lightweight advanced endoatmospheric KKV design and an airborne X-band radar, as shown by the thin outer ring around the ABI launch location along the Iraq-Iran border in Figure 18, unless the ABI platform flies over Iranian territory. The inner circle at this location corresponds to the ABI intercept range with a 1,000 kg ABI carrying the baseline endoatmospheric KKV and using space-based infrared sensors with 1 km pixel footprints.

The ABI intercept ranges in Figures 19 and 20 are drawn for ICBMs launched from central Iran, which represents a worst-case detection geometry

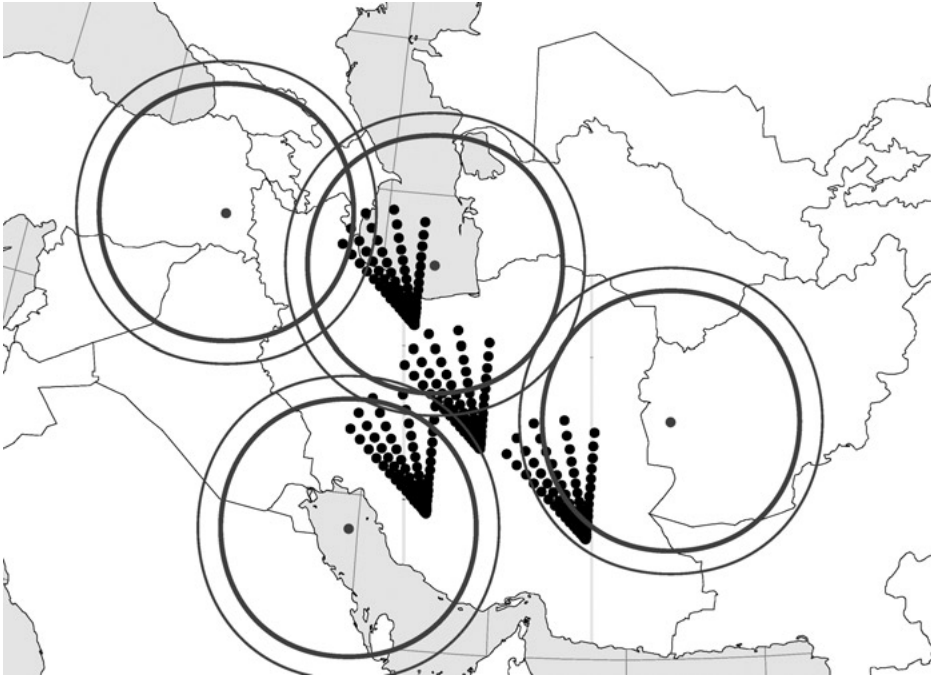


**Figure 20:** ABI intercepts against 180-sec solid-propellant Iranian ICBMs.

although not necessarily the longest-range intercept geometry. In this case, a 1,500 kg ABI with the baseline exoatmospheric KKV using space-based infrared sensors with 1 km pixel footprints should be able to intercept 240-second (and 290-second) liquid-propellant ICBMs from launch locations outside Iranian airspace, as one can see from Figure 19. However, three or more launch locations would be required if Iran spread its hypothetical ICBM force across its territory or if U.S. intelligence is unable to localize all possible ICBM launch locations. ABI intercept of a 180-second solid-propellant ICBM is not possible unless more rapid target detection and tracking is available, even with the 48 kg advanced exoatmospheric KKV (the thin outer circles in Figure 20). ABI launch platforms would have to move closer to Iranian airspace, or possibly fly over Iranian airspace, to have high confidence that solid-propellant ICBMs could be intercepted.

In summary, typical intercept ranges for medium-range, intermediate-range, solid-propellant ICBMs, and liquid-propellant ICBMs are between 0–200 km, 400–650 km, 430–600 km, and 600–1,000 km, respectively. For large

states such as Iran, space-based infrared detection and tracking is the best sensor option. However, for small states such as North Korea airborne X-band radar can add significantly to the ABI flight time, thus enabling intercepts that would otherwise be infeasible without flying over North Korean airspace. Finally, the baseline KKV designs illustrated in Table 3 provide satisfactory intercept capability under most circumstances, but stressing threats such as short burn time MRBMs (Scud B) and solid-propellant ICBMs require lighter KKV's similar in mass to the advanced KKV's illustrated in Table 3.

### **ABI Force Size**

The required size of the ABI arsenal is determined by the number of ABI missiles that must be launched at each booster target to obtain a high intercept probability, multiplied by the estimated number of missiles in the opponent's arsenal. To this one must add the number of missiles that are airborne at any given time in areas from which no missiles are launched, that is, absentee ABIs, and the number of missiles needed for operational test and evaluation, and spares. The approximate number of ABI launch platforms for an effective force is determined by multiplying the number of ABIs that must be launched at each target by the maximum number of ballistic missiles that can be launched from a single ABI defended area in the time it takes to replace ABI launch platforms that have exhausted their interceptors (i.e., several hours), multiplied by the number of ABI defended areas required to cover all possible launch locations in the country of concern, divided by the carrying capacity of each ABI launch platform, and, finally, multiplied by the ratio of the number of ABI launch platforms required to support one in the air 24 hours a day, 7 days a week. Note that concentrating mobile MRBM launchers for large salvo attacks makes them more vulnerable to air attack and, hence, is not necessarily a preferred offensive tactic. Moreover, if their movement is detected in time, ABI launch platforms can be concentrated against them. ICBM launch sites are likely to be fixed, at least for first generation ICBMs.

To illustrate this arithmetic, assume four ABIs must be launched at each booster target to achieve a high probability of kill and that the maximum salvo launch capability is 20 MRBMs or 10 ICBMs. In this case, approximately 40–80 ABI, possibly with a mixture of endoatmospheric and exoatmospheric KKV's, would have to be airborne in each ABI defended area to ensure that no salvo launch from any area could saturate the defense. Depending on the geography and whether the missile threats are principally from medium, intermediate, or intercontinental-range ballistic missiles, anywhere from one to three ABI defended areas would be required to adequately cover the territory of interest.

Three defended footprints, for example, would require approximately 120–240 ABIs airborne at all times.

The number of ABI launch platforms required to support this presence is determined by the carrying capacity of each platform and its airborne endurance. If we assume that bombers or other large aircraft can carry twenty 1,500 kg or 1,000 kg ABI, fighter aircraft can carry four 1,000 kg ABI, and a large long-endurance UAV like the Global Hawk can carry one 1,000 kg ABI, then up to 12 bomber-sized aircraft, 60 fighter aircraft, or 240 UAVs airborne, or some mix of these, would have to be airborne at all times in the three defended areas. The airborne endurance for bomber-sized aircraft, fighters and long-endurance UAVs like the Global Hawk is approximately 12, 8, and 24 hours, respectively. If one assumes one additional launch platform on the ground for a spare in case of maintenance problems, then three bombers, four fighters, or two UAVs would be required to support one airborne 24 hours a day for extended periods of time. Therefore, the total inventory of launch platforms to keep 240 ABI airborne at all times would be roughly 36 heavy bombers or similar large aircraft, 240 fighter aircraft, 480 UAVs, or some mix of these platforms. A mix is preferable to take advantage of the different payload capacities, endurance, and vulnerability of each platform. In any case, this is a large force! Clearly, lightweight ABI are desirable to increase the carrying capacity of each launch platform, thereby minimizing the cost for procuring and operating the launch platform force.

The number of ABI missiles required for an opposing arsenal of 100 missiles is 400 (assuming four ABI are launched at each target), plus 160 that are airborne in two of the three ABI defended areas where missile launches might not occur and perhaps 20 percent more for spares. Thus, the total ABI inventory in this example would be about 700 ABI missiles for a threat of 100 ballistic missiles and a geography that requires three zones to adequately cover all possible launch locations. Clearly, one must tailor this arithmetic to different circumstances.

Estimates for the overall acquisition cost for such a force are necessarily rough because the cost for the different elements is not well known. Nevertheless, the overall acquisition cost will be driven by the launch platform cost and the cost of the airborne radar, if it is part of the sensor architecture. The individual ABI missiles are relatively inexpensive (estimated here to cost about \$3 million each based on analogy with Air-Launched and Sea-Launched Cruise Missiles, which cost about \$2 million and \$1 million each, respectively). Therefore, an inventory of 700 ABI would cost approximately \$2.0 billion. If we assume new launch platforms are purchased, that is, they cannot be obtained from another part of the Air Force or Navy, then heavy bombers of the B-1B

type, fighters similar to the F-15E, and UAVs similar to the Global Hawk would cost approximately \$300 million, \$20–\$30 million, and \$16–\$20 million each, respectively.<sup>43</sup> The cost to fill three orbits 24 hours a day for 20-missile salvo launch threats is approximately \$11 billion, \$5–7 billion, and \$8–10 billion for the bomber, fighter and UAV forces, respectively. If two airborne radar orbits are maintained 24 hours a day, this would require an inventory of approximately eight aircraft. Assuming these radar are similar in cost to the E-3 AWACS (approximately \$400 million each), this would add another \$3.2 billion to the acquisition cost.

Therefore, the total acquisition cost for an airborne boost-phase ballistic missile defense system, not including space-based sensors, would be roughly \$10 to \$16 billion for 700 ABI missiles and enough launch platforms to cover three defended areas 24 hours a day with enough ABIs to handle salvo launch threats of up to 20 missiles and enough airborne X-band radar to maintain two radar orbits 24 hours a day near a country of concern. This does not include operating costs or research and development costs. If bomber or fighter aircraft could be drawn from other parts of the Air Force or Navy, this would reduce the acquisition cost considerably. These numbers are very approximate. More refined estimates are needed if ABI systems are considered in future U.S. ballistic missile defense plans.

## **BOOST-PHASE COUNTERMEASURES**

Relatively few countermeasures exist against boost-phase ballistic missile defenses. Clearly lightweight decoys and other penetration aids that challenge midcourse ballistic missile defense systems do not interfere with boost-phase defense. The two obvious countermeasures are missiles with short boost times and missiles that can maneuver during their boost phase. Both of these countermeasures have been taken into account in this analysis. Solid-propellant missiles, for example, the 180-second ICBM examined in this analysis, stress boost-phase intercepts. However, ABIs still have substantial capability if light-weight advanced KKV's can be designed. If fast burn solid-propellant ICBMs are deployed of the sort hypothesized during the US Strategic Defense Initiative in the mid-1980s with boost times as short as 100 seconds, then boost-phase intercept capability would be severely compromised unless ABI launch platforms fly over the opponent's territory.

Ballistic missiles launched against targets at less than their maximum range have excess fuel that can be used for boost-phase maneuvers. These are not rapid maneuvers—which probably would be ineffective for avoiding the

more agile boost-phase KKV—but relatively slow maneuvers that move the predicted intercept point as several hundred kilometers from the original predicted intercept point determined at the time the ABI booster burns out. This error must be removed by the KKV. The kill vehicle used in this analysis has the ability to change its velocity by 2.0 km/sec, an amount sufficient to compensate for most first generation booster maneuvers. If greater booster maneuvers are deemed feasible, more KKV divert capability will be required. Therefore, this countermeasure can be managed in a straightforward manner.

Beyond these two countermeasures, one can imagine flares, sounding rockets with similar acceleration profiles to larger ballistic missiles, salvo launches, and boosters designed to fractionate during their last stage so the defense is presented with multiple targets during the intercept end game. Most of these countermeasures would not be effective. Flares can be distinguished by their low emitted infrared power and their “color.” Sounding rockets can be designed to accelerate like larger missiles; however, their infrared signature is smaller than that from large rocket motors, especially during first stage flight. This countermeasure might delay an ABI launch until the infrared signature could be determined, thus eliminating the benefits of early launch detection associated with airborne radar. However, it would not fundamentally defeat the system. Salvo launches could saturate the detection and tracking architecture or deplete the supply of available ABIs within range of the salvo launch. Again, this is easily countered by fielding more sensors and interceptors, at some cost. Since interceptors can be launched in rapid succession, even from the same launch platform, it is difficult to imagine that salvo launches of as many as 10 to 20 missiles could defeat a well designed ABI deployment. Finally, missiles with fractionated last stages are probably beyond the capability of emerging missile states and clearly would have to be tested before they are deployed. Boost-phase proponents have suggested interceptors with fractionated KKV as a defensive counter-countermeasure, but such devices would be technically challenging to build.<sup>44</sup> Hence, this countermeasure and its defensive response seem fanciful at the current time.

## **ABI OPERATIONAL AND POLITICAL CONSTRAINTS**

Several operational limitations make the ABI concept less than ideal for missile defense, although none are so constraining as to eliminate this boost-phase defense option. First, for national missile defense against large, inland states like Iran, access to neighboring airspace is required (e.g., in the case of Iran, Turkish, Turkmenistan, and Afghanistan airspace, as well as the airspace over the Caspian Sea and the Persian Gulf). This presents problems if neighboring

states fail to cooperate. ABI systems could defend against North Korean ICBM threats—the easy case for boost-phase missile defense—from international air space over the Sea of Japan. Similarly, airborne X-band radar could be located in international airspace in the case of North Korea but larger states like Iran would require access to neighboring airspace. Space-based infrared sensors clearly are preferable in this regard.

Second, access to the opponent's airspace may be required for short burn-time ICBMs (i.e., burn times less than 180 seconds) and short-range MRBMs. Stationing ABI launch platforms over an opponent's territory violates its sovereignty and constitutes an act of war because these platforms are armed aircraft. If ABI launch platforms are located outside the opponent's airspace, with plans to penetrate their airspace soon after hostilities commence, then short-burn missiles launched at the start of a war would get a free ride through the defense, thus creating pressure on both sides to preempt. However, ABI launch platforms can enter enemy airspace within minutes after a conflict begins, thereby providing a useful defense in scenarios where, for example, ballistic missiles armed with weapons of mass destruction are held in reserve to be launched only when the survival of the regime is threatened. Still, short-burn missiles could exert considerable political leverage before a war starts if the defense cannot defend against the first few missiles launched.

Third, ABI platforms in and around an opponent's airspace may not survive enemy air defenses. This poses a difficult challenge if ABI platforms are required to loiter over hostile territory, although it may also be a problem if the launch platform orbits over neighboring airspace. Standoff ranges of 100–150 km would keep the launch platform out of range of enemy surface-to-air missiles; however, air defenses (F-15C/D and AWACS aircraft) would be required to protect the ABI launch platforms from enemy fighters that enter neighboring airspace. This increases the operational cost of deploying ABI systems. Using high-altitude UAVs flying above 60,000 feet reduces their vulnerability; however, it does not make them immune to advanced fighters with advanced air-to-air missiles. Stealth technology would help reduce this vulnerability significantly, but this substantially increases launch platform cost. After a war starts, the air defenses of small states can be suppressed, making ABI platform survival less of an issue. Again, scenarios where an opponent actually launches, as opposed to threatens to launch, ballistic missiles armed with nuclear, biological, or chemical weapons often occur late in a war. In these scenarios, ample time should exist to establish air superiority over the opponent's territory. Conventionally-armed ballistic missiles, on the other hand, may be launched early in a conflict, as was the case in the 1991 Gulf War with Iraq, with their concomitant political costs.

Fourth, keeping aircraft airborne for months on end would be costly, although it can be, and has been, done for periods extending from several months to over a year. This is not a trivial air operation. However, it is no more complex than the air operations the United States routinely plans for theater air defense. Therefore, ABI systems could be available for weeks, if not months, on end, 24-hours a day, 7 days a week. However, such a defense could not be maintained for years on end due to the operational costs. Consequently, airborne boost-phase ballistic missile defense is a crisis or wartime defense and would not be effective against accidental or unauthorized missile launches unless they occurred in the midst of a crisis or war.

Fifth, the short reaction time required to make any boost-phase defense, including airborne boost-phase defense, effective implies that there is little time for high-level decisions regarding the release of boost-phase interceptors. At first glance, this appears to be a serious concern. However, one should bear in mind that ABI release authority is very different from nuclear weapon release authority. No explosive weapons are involved. Boost-phase interceptors fired at fictitious targets would burn up in the atmosphere, posing little threat to humans on the ground. Moreover, boost-phase defense is very different from other situations where military and civilian operations intermingle. False warning of a missile launch is not likely. There are very few civilian rocket launches that mimic a ballistic missile launch; unlike air defenses, for example, where identifying friend from foe and combatant from noncombatant aircraft is a serious issue, or ground attack where distinguishing hostile from friendly vehicles contributes to tragic friendly-fire incidents and collateral damage to noncombatants in every war. Space-launch vehicles might be confused with missile launches, but they are almost always launched from designated launch sites with days of advance notice in peacetime. In the event they are not, as was the case with the August 31, 1998 North Korean satellite launch attempt, such rockets may be shot down in a crisis or war. Therefore, predelegating intercept launch authority to field commanders, which is required to make any boost-phase defense effective, entails acceptable risks, unlike the case of predelegating launch authority to field commanders for nuclear weapon use.

Finally, forward deployment of ABI systems could appear to an opponent to be escalatory. This dilemma arises with the forward deployment of almost any military system. There is no particular reason why deploying boost-phase missile defenses would be more destabilizing than deploying other air, naval, or ground forces forward in a crisis. Any military action of this sort entails the risk of escalation, as well as the potential to de-escalate a crisis. The usual sense in which ballistic missile defense is thought to be destabilizing occurs when a preemptive attack can degrade the opponent's ballistic missile force to the



point where the defense can handle the “ragged” retaliatory strike. Emerging missile states certainly would worry about preemptive attacks against their ballistic missiles by U.S. conventional, and perhaps nuclear, forces. The presence of boost-phase defenses may signal the impending attack. However, regional opponents have little to gain by launching nuclear, biological, or chemical ballistic missiles out of fear of losing this capability when boost-phase defenses are forward deployed because to do so would be an act of suicide at a point early in an evolving crisis when the leadership may still hope to avoid war.

## **DOES AIRBORNE BOOST-PHASE MISSILE DEFENSE THREATEN RUSSIA OR CHINA?**

If ABI systems are effective against theater- and intercontinental-range ballistic missiles launched from emerging ballistic missile states, they might also be effective against Russian and Chinese ICBMs and SLBMs, thus provoking political, if not military, responses from these two major nuclear powers. In fact, ABI systems do not pose a realistic threat to either Russian or Chinese strategic ballistic missiles.

Figure 21 illustrates the ABI coverage of potential Russian ICBM and SLBM, and Chinese ICBM launch locations. The ground-traces for ICBM and SLBM boosters launched from representative locations toward targets on the U.S. east and west coasts also are illustrated. The ABI intercept ranges are based on ABI launch delays using a space-based infrared detection and tracking sensor with 1 km pixel footprints (airborne radar cannot operate close enough to all possible Russian or Chinese launch locations). The intercept range for a 1,500 kg ABI armed with a 48 kg advanced exoatmospheric KKV against Russian SS-25 solid-propellant ICBMs (which are being replaced by the shorter burn time SS-27) is estimated to be at most 600 km (see Table 5); the intercept range against Russian liquid-fuel SLBMs such as the SS-N-23 (with a boost time of 250 seconds) is estimated at less than approximately 830 km (the future Russian SS-NX-28 SLBM may contain solid propellant and, hence, have a shorter burn time); and the ABI intercept range against the Chinese DF-5 liquid-fuel ICBM is estimated to be at most 800 km (although the future Chinese DF-31 solid-propellant ICBM has a shorter boost time). These intercept ranges are illustrated in Figure 21 for ABI launch locations close to potential Russian and Chinese launch locations.

As one can see, it takes about five ABI orbits to cover Russia’s ballistic-missile submarine bastions near its territory. If, in the future, Russia’s SLBM force is located entirely with the Northern Fleet, this figure drops to around

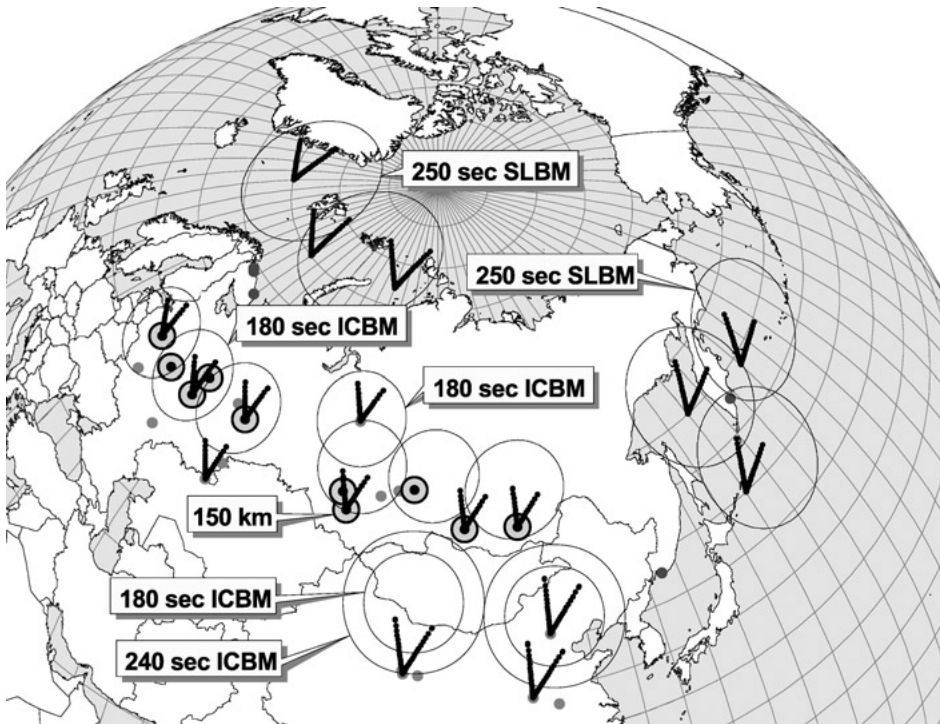


**Figure 21:** ABI capability against Russian and Chinese strategic missiles.

two or three ABI orbits. Despite a preference for basing submarines in bastions, Russian missile-carrying submarines can deploy into the open ocean, with perhaps some greater risk from U.S. antisubmarine warfare. In this case, approximately 20 ABI orbits would be required to cover all possible SLBM launch locations in the North Atlantic, and 30 would be required for all possible launch locations in the North Pacific—unless the United States can localize Russian submarines by tracking them in the open ocean.<sup>45</sup> If Russia deploys single-warhead ICBMs in former SS-18 and SS-19 silos, and mobile SS-27 ICBMs at up to 10 garrisons used in the past for mobile SS-25 ICBMs, at least seven additional ABI orbits would be needed to cover all possible ICBM launch locations. The smaller shaded circles (with a radius of 150 km) in Figure 21 represent the approximate area into which mobile ICBMs could deploy within 10 hours after leaving their garrison. Larger deployment areas may be possible, but logistical constraints eventually limit their size. Clearly, as mobile ICBM deployment areas grow in size, more ABI orbits would be required.

Therefore, the United States would have to keep ABI launch platforms aloft continuously in at least 10 areas to cover likely Russian ICBM and SLBM launch locations, and potentially three to four times this number if Russia sends its missile-carrying submarines into the open ocean. This would be a daunting task! Aircraft and UAVs may not have enough fuel to reach these locations from distant allied airfields. More importantly, ABI launch platforms, sensor aircraft, and airborne tanker support would be vulnerable to Russian air defenses. While it is plausible to think of suppressing the air defenses of a weak state, suppressing Russia's strategic air defense system is an entirely different matter, even with the current degraded state of Russia's air defenses. In addition, the airfields from which ABI operations originate would be vulnerable to Russian attack because they are few in number and relatively easy to identify. Emerging ballistic-missile states would have difficulty carrying out such attacks. Finally, Russian salvo launches could be quite large and would make any residual airborne boost-phase system quite ineffective. Hence, an ABI boost-phase ballistic missile defense system would pose very little threat to Russia's ICBMs and SLBMs for operational reasons and not because an ABI could not intercept a Russian strategic missile if it is within range.

Airborne boost-phase systems may pose more of a threat to Chinese strategic missiles because China has fewer ICBM launch sites, the boost time for the Chinese DF-5 ICBM is relatively long, and China has few, if any, operational SLBMs that can threaten the United States (not to mention their vulnerability to U.S. anti-submarine warfare). However, ABI platforms still would have to penetrate deep into Chinese airspace to cover all possible ICBM launch locations, thereby exposing themselves to increasingly sophisticated Chinese air defenses. The distances from ABI bases to reasonable orbit points are large, making the airborne operation difficult to sustain. Chinese attacks against ABI airfields also are a possibility. Finally, China is in the process of modernizing its strategic arsenal with solid-propellant mobile DF-31 ICBMs. Thus, the number of ABI sites required to cover all possible Chinese ICBM launch sites will grow substantially in the next decade. Therefore, the threat posed by an ABI system to China's strategic missiles is not very great. However, ABI systems might pose a threat to Chinese theater-range missiles aimed at Taiwan from across the Taiwan Strait—although China could still threaten Taiwan with longer-range missiles launched from deeper inside the mainland. Consequently, while ABI systems pose little threat to China's future strategic arsenal, the deployment of ABI systems could complicate Sino-U.S. relations.

Finally, it is interesting to note that a Russian ABI system would not threaten U.S., French, British or Chinese strategic forces, for the same reasons cited above. Therefore, the British and French concern during the Cold

War—that U.S. missile defenses would spur the deployment of Russian defenses which undermine their strategic deterrent—is without substance in the case of ABI boost-phase defenses because France and Great Britain rely on SLBMs for their strategic deterrent and Russia simply cannot mount or sustain the airborne operation required to put these assets at risk. This creates the interesting possibility that the United States, Russia, and interested NATO countries could collaborate on the development, and possible deployment, of ABI defenses without giving rise to suspicions about each other’s strategic intent.

### **COMPARISON WITH THE APS BOOST-PHASE MISSILE DEFENSE STUDY**

This analysis is largely consistent with the recently published American Physical Society report on boost-phase ballistic missile defense. Both studies agree that timely detection and tracking is critical to boost-phase missile defense and that space-based infrared sensors will play a key role. This study highlights the importance of airborne X-band radar for rapid launch detection and tracking, especially for favorable geographies like North Korea. The APS Study did not consider airborne X-band radar. Both studies agree that boost-phase KKV’s with total divert velocities of at least 2.0 km/sec are required for effective boost-phase intercept against ICBMs and that masses in the range of 50–100 kg for such KKV’s should be technically feasible in the next decade. They also agree that boost-phase intercept from terrestrial launch platforms, airborne platforms in particular, is technically feasible against relatively slow burning liquid-propellant ICBMs.

However, the conclusions differ with respect to solid-propellant ICBMs. The APS study finds that:

Boost-phase defense of the entire United States against solid-propellant ICBMs, which have shorter burn times than liquid-propellant ICBMs, is unlikely to be practical when all the factors are considered, no matter where or how interceptors are based. Even with optimistic assumptions, a terrestrial-based system would require very large interceptors with extremely high speeds and accelerations to defeat a solid-propellant ICBM launched from even a small country such as North Korea.<sup>46</sup>

Contrary to this conclusion, the current study finds that solid-propellant ICBMs are not beyond the reach of airborne interceptors. Clearly, short burn missiles create stressful timelines for boost-phase defense. Solid-propellant ICBMs, in particular, are difficult targets. However, there is no “knee in the curve” beyond which airborne boost-phase intercept is no longer feasible. To

some extent this different conclusion can be traced to different input assumptions in the two analyses.

On the physics, both studies agree. However, the APS study uses more conservative input assumptions. For example, the APS Study bases the burn time for solid-propellant ICBMs on U.S. solid-propellant SLBMs, which have slightly shorter (170-second) nominal burn times compared to the U.S. and Russia solid-propellant ICBMs used in this study with 180-second nominal burn times. The APS study also assumes that it takes approximately 45 seconds to detect and track solid-propellant ICBMs after launch. This study has determined that solid-propellant ICBMs can be detected and tracked within 29 seconds after launch in the case of North Korea using an airborne X-band radar and within 37 seconds after launch using space-based infrared sensors with a 1 km pixel footprint. The shorter detection and tracking time associated with space-based infrared sensors comes about because this study assumes that initial target heading errors can be removed during the interceptor's 20-second boost phase prior to KKV release, thus allowing the ABI to be launched a few seconds earlier. Airborne missiles can also accelerate faster and, hence, have higher average flight speeds relative to surface-based interceptors (upon which the APS study focused) because the drag force is lower at high altitudes. The net result is that the ABIs examined in this study have approximately 25 seconds more flight time against solid-propellant ICBMs launched from North Korea than comparable intercepts in the APS study.<sup>47</sup> This translates into intercept ranges that are approximately 100 km greater than the APS intercept ranges. One should also keep in mind that this study invoked higher-speed ABIs using light-weight advanced KKV's before concluding that 180-second solid-propellant ICBMs could be intercepted.

Even with the more optimistic assumptions used in this study, solid-propellant ICBMs and short-range MRBMs are very difficult targets and their successful intercept will require sensor architectures that are designed to push the detection and tracking time as low as possible and interceptors with the highest possible speed (determined here to be around 6.0 km/sec ideal velocity) through the use of light-weight KKV's and large (1,500 kg) airborne missiles. While 50 kg KKV's stretch what is currently possible, solid-propellant ICBMs stretch what is currently possible in terms of offensive threats. Neither may be far fetched 10 years from now.

Finally, it is important to note that airborne interceptors have the distinct advantage that they can always be moved closer to the suspected launch site if the ABI intercept range is marginal, albeit with the requirement to gain access to neighboring airspace or to fly near, if not over, the opponent's airspace, with increased concern for launch platform survival. If the threat is

serious enough, these risks may be acceptable. For example, in the case of North Korea, solid-propellant ICBMs could be intercepted if the ABI launch platform orbited over Chinese airspace and, perhaps, if orbited over Russian airspace north of Vladivostok. Ground-based interceptors do not have this option and naval interceptors are limited to navigable waters. Moreover, in some scenarios an opponent's air defenses may be seriously degraded by the time ICBM launches actually occur. If airborne platform survival is of paramount concern, one can employ low-observable launch platforms, at increased cost. Still, the issue is not one of ABI technical capability against short burn time boosters but rather whether the defense is worth the cost. Even if one assumes airborne platforms are stationed far enough outside enemy airspace to be reasonably safe from air defense threats, ABIs still can intercept most solid-propellant ICBM trajectories using 1,500 kg ABIs and 50 kg KKV's with actual flight speeds of approximately 5.5 km/sec (6.0 km/sec ideal velocities). Such interceptors are not very large and, while their speed is high, reasonable missile designs based on current technology should be able to achieve this performance.

Finally, one should note that the most important considerations that affect individual preferences for boost-phase ballistic missile defense often are not technical, but rather have to do with operational concerns, different threat assessments, and cost. These concerns are largely outside the scope of this study. Therefore, one should not be surprised if different analysts, even technical analysts, come to different conclusions regarding the wisdom of pursuing one type of missile defense over another.

## **CONCLUSION**

Boost-phase interceptors light enough to be launched from aircraft appear to be technically feasible for both theater and national missile defense. Within the next decade, endoatmospheric KKV's with the capability to home on maneuvering boosters (i.e., with 1.0 km/sec of divert) probably can be built with a mass between 30–55 kg and exoatmospheric KKV's with 2.0 km/sec of divert probably can be built with a mass between 50–90 kg. Early ballistic missile launch detection and tracking is crucial for an effective boost-phase defense. Space-based infrared sensors and airborne X-band radar both appear to offer timely detection, resulting in ABI intercept ranges against IRBMs, solid-propellant ICBMs, and liquid-propellant ICBMs between 400–650 km, 430–600 km, and 600–1,000 km, respectively. An effective boost-phase defense against MRBMs requires airborne X-band radar for early launch detection and tracking. In this case, ABI intercept ranges on the order of 100–230 km may be achieved against

MRBMs with boost times below 100 seconds. In general, airborne interceptors are the only form of terrestrial boost-phase defense that can be effective against very short burn time ICBMs and MRBMs because, if necessary, they can fly over an opponent's territory.

In addition, while ABI systems offer the prospect of an effective defense against emerging ballistic-missile threats, including threats such as chemical or biological submunitions, they pose very little threat to the strategic nuclear forces of the five major nuclear powers. Thus, ABI systems will appear threatening to emerging missile states, yet not destabilizing to the major nuclear powers—states with which the United States has many interests in common. To the extent one takes the rhetoric of sharing U.S. ballistic missile defense technology with other countries seriously, ABI systems may be the most transferable type of ballistic missile defense because they cannot be used directly against the United States. The technology upon which ABI systems are based may be sensitive, but operational ABI systems cannot threaten U.S. strategic forces. For all of these reasons, the United States should pay more attention to this boost-phase defense option than currently is the case.

The principal drawbacks associated with ABI systems are that they offer no protection against accidental or unauthorized Russian or Chinese missile launches, or for that matter accidental or unauthorized launches from emerging missile states unless they occurred in the midst of a crisis or war when ABI systems would be on station. Moreover, they are expensive to operate and they are inherently less robust to those offensive countermeasures that increase the weight of the KKV—for example, large ICBMs with lots of excess maneuver capability that require heavy KKV with divert velocities above 3.0 km/sec and, hence, heavy interceptor missiles—because of the maximum weight limits for air-launched missiles. Again, ABI launch platforms can move closer to potential missile launch sites to compensate for the slower speeds associated with heavier KKV if necessary. However, none of these limitations is so severe as to eliminate the ABI option from consideration as a viable component of a future U.S. missile defense architecture. In fact, compared to the limitations inherent in all boost-phase missile defense concepts, airborne intercept remains one of the most attractive options.

This analysis has concerned itself principally with the technical feasibility and operational effectiveness of airborne boost-phase intercept. The larger questions of the priority that any form of ballistic missile defense should receive relative to other important U.S. security concerns (e.g., countering terrorism, U.S. conventional force modernization, etc.) and the cost-effectiveness of ABI compared to other forms of ballistic missile defense are not addressed here.

## NOTES AND REFERENCES

1. A prototype airborne laser carried aboard a 747 aircraft is currently under development, with deployment expected some time between 2007 and 2010. For a technical analysis of its capabilities see the report of the American Physical Society (APS) Study Group entitled *Boost-Phase Intercept Systems for National Missile Defense: Scientific and Technical Issues*, July 2003 ([http://www.aps.org/public\\_affairs/popa/reports/nmd03.html](http://www.aps.org/public_affairs/popa/reports/nmd03.html)); (29 March 2004); and Geoffrey Forden, "Airborne Laser: Shooting Down What's Going Up," Center for International Security And Cooperation, Stanford University, September 1997. Space-based lasers have been under consideration for many years, however, they will not be technically feasible until 2015–2020, at the earliest.
2. See, APS Study, *Boost-Phase Intercept Systems for National Missile Defense*, July 2003, Section 10.3.
3. Airborne infrared sensors operating in the short or medium-wave infrared band have an angular resolution on the order of  $10^{-5}$  radians for 30 cm optics and, hence, will have track resolutions on the order of six meters from ranges of 600 km. Such track accuracies would allow rapid target azimuth determination and might facilitate booster typing.
4. Space-based LIDAR systems, and airborne LIDAR systems if they can fly at altitudes above 60,000 feet and get within 600 km of their targets, may play an interesting role in boost-phase missile tracking. However, such sensors were not examined in this study.
5. For a detailed treatment of these issues see Frederick S. Simmons, *Rocket Exhaust Plume Phenomenology*, The Aerospace Corporation Press, El Segundo, CA, 2000.
6. An NEI of  $10^{-14}$  W/cm<sup>2</sup> represents a conservative noise figure in the 2.7  $\mu$ m band for a 30 cm aperture telescope.
7. APS Study, *Boost-Phase Intercept Systems for National Missile Defense*, July 2003, Section 10.1.
8. *Ibid.* Sections 10.1.2 and 10.1.3.
9. If one assumes subpixel resolution for the space-based infrared sensor, which should be possible if the image spot is comparable to the pixel dimension on the focal plane array, then the approximate target heading can be determined more rapidly than has been assumed here. After initial detection, the sensor can collect tens of frames of data on the moving target by staring at the detected spot in less than one second.
10. Heading errors, for the purpose of this analysis, are determined in a simple-minded manner by taking half of the pixel footprint dimension ( $\pm 0.5$  km for a 1 km  $\times$  1 km footprint) and dividing it by the downrange distance the target missile flies. More accurate calculations would take the lateral position, velocity, and acceleration uncertainties produced by the tracking filter as a function of time after initial detection to determine when the ABI could be launched.
11. This  $\Delta V$  requirement is calculated based on the lateral distance error produced by a heading error, which is determined by the downrange distance the missile flies as a function of time and the sensor resolution. Assuming proportional navigation during this portion of the ABI flight and normal intercept trajectories, the divert requirement is given by where

$$\Delta V = \frac{\theta \cdot R \cdot v_t}{v_i} \cdot \frac{N}{(N-1)t},$$



where  $\theta(t)$  is the heading error as a function of time (i.e., the resolution of the sensor divided by the downrange distance the missile travels as a function of time after initial detection),  $R$  is the nominal intercept range (approximately 600–800 km for ICBM targets),  $v_t$  is the average target speed (approximately half the ballistic missile burnout speed),  $v_i$  is the interceptor speed (approximately 5 km/sec for ABIs),  $N$  is the navigation ratio for proportional navigation (assumed here to be 4), and  $t$  is the time to intercept which depends on the boost-phase duration of the target ballistic missile.

12. The tracking time depends on the exact range of the trajectory compared to the missile's maximum range because this determines how much propellant is available for lofting the missile. Table 1 is based on conservative lofted trajectories. However, worse trajectories could be constructed if a long-range missile such as the Taepo Dong 2 is used to attack a target at very short range. In this case, the initial missile trajectory could be nearly vertical and the tracking delays would be longer than those given in Table 1. Of course, the reentry vehicle would have to be designed to handle the higher reentry speeds associated with these lofted trajectories.

13. Designing ABI boosters with a sustainer motor that continues to provide thrust after the main booster burns out would help reduce the KKV divert requirement at the expense of interceptor speed. A system tradeoff study would be required to determine whether this is beneficial. This analysis assumes that the KKV must carry sufficient fuel to correct for maneuvering targets on its own.

14. For an analysis of theater-range ballistic missile targets that predicts several kilometer predicted intercept point errors, see R.C. Laco, D.C. Johannsen, K.L. Zondervan, and Col. T. Fitzgerald, "Sensor Fusion Applications In The Airborne Interceptor (ABI) Program," presented at the 8th National Symposium on Sensor Fusion, 1995.

15. See Merrill I. Skolnik, *Introduction to Radar Systems*, 3rd ed., New York: McGraw Hill, 2001, pp. 89–90.

16. See *Boost-Phase Intercept Systems for National Missile Defense*, op. cit., Section 10.2.2.

17. The time required to pass through the elevation beam width depends on the radar elevation beam width, the missile's vertical speed, and the range from the radar to the target. Faster missiles (e.g., solid-propellant ICBMs and some MRBMs) have greater vertical velocities and reach an altitude where they appear above the radar horizon earlier than liquid-propellant ICBMs. MRBMs can have high elevation rates because frequently they are detected at shorter ranges (e.g., 250–400 km) than ICBMs (i.e., 400–700 km). The notional 180-second solid-propellant, 240-second liquid-propellant, and 290-second liquid-propellant ICBMs examined in this analysis have elevation rates of approximately 1.0 mrad/sec, 0.75 mrad/sec, and 0.60 mrad/sec, respectively, for an airborne radar at a detection range of 400 km. Scud B, Scud C, and No Dong MRBMs launched from North Korea have elevation rates when viewed by an ABR south of the DMZ between approximately 0.5 to 1.0 mrad/sec for detection ranges varying from 230 to 330 km.

18. See David K. Barton, *Modern Radar System Analysis*, Artech House, 1988, pp. 523–530.

19. Airborne X-band radar actually can detect solid-propellant ICBMs at ranges less than the horizon (i.e., less than 400 km) within as little as 12–15 seconds after launch, much faster than space-based infrared detection, because the radar has line of site to the target and it takes only a short time for the target to exceed the radar's Doppler

notch. This favorable geometry occurs for North Korean launches but would not occur for larger countries where the airborne radar cannot get as close to the missile launch site. However, even with such early launch detection, accurate tracking cannot begin until the target missile has climbed about half a beam width above the horizon. As it turns out, this longer track delay, when added to the shorter detection delay for solid propellant ICBMs yields the same total launch delay given in Table 1.

20. See David R. Vaughan, Jeffrey A. Isaacson, and Joel S. Kvitky, *Airborne Intercept: Boost and Ascent-Phase Options And Issues*, RAND Corporation, MR-772-AF, 1996, pp. 16–17.

21. Clementine sensor suite data can be found at (<http://www.cmf.nrl.navy.mil/clementine/sci.clem.html>) (29 March 2004) and (<http://www-phys.llnl.gov/clementine/sensors/sensors.html>) (29 March 2004).

22. K. Bryant, C. Knight, and R. Hurtz, “Planetary Lander Vehicles Utilizing LEAP Technology,” AIAA 94-2748, 30th AIAA/ASME/SAE/ASEE Joint Propulsion Conference, June 27–29, 1994.

23. Tank ullage is assumed to be 15 percent and propellant expulsion efficiency is assumed to be 97 percent.

24. The data for composite pressure tanks came from Structural Composite Industries (<http://www.scicomposites.com/>) (29 March 2004).

25. Note that a simple theoretical argument based on hoop stress for cylindrical tanks at constant pressure would predict that the mass-to-volume ratio would remain constant as a function of tank volume. This is not quite accurate because small tanks cannot be designed with arbitrarily thin walls and, hence, they tend to have higher mass-to-volume ratios, as illustrated in Figure 6.

26. The data for titanium pressure and propellant tanks is from Pressure Systems Incorporated ([http://www.psi-pci.com/Data\\_Sheets1\\_main.htm](http://www.psi-pci.com/Data_Sheets1_main.htm)) (29 March 2004).

27. This tank is scaled up from the 2000 psi S12962 propellant tank found on (<http://www.ardeinc.com/liquid.html>) (29 March 2004).

28. For developments and applications of small pump-fed divert rocket engines see: John C. Whitehead, *Bipropellant Propulsion with Reciprocating Pumps*, Lawrence Livermore National Laboratory, UCRL-JC-114530, June 16, 1993; John C. Whitehead, *Mars Ascent Propulsion Options for Small Sample Return Vehicles*, Lawrence Livermore National Laboratory, UCRL-JC-127445, May 12, 1997; and J.C. Whitehead, *Hydrogen Peroxide Gas Generator Cycle with a Reciprocating Pump*, paper AIAA 2002-3702 presented at the 38th AIAA/ASME/SAE/ASEE Joint Propulsion Conference, July 7–10, 2002.

29. L.C. Ng, E. Breitfeller, and A.G. Ledebuhr, *An Optimal  $t$ - $\Delta V$  Guidance Law for Intercepting a Boosting Target*, Lawrence Livermore National Laboratory, UCRL-JC-148995, June 30, 2002, p. 3.

30. See Steve Brown, et al., *Interceptor Concepts for the U.S. UAV Program*, presented at the 5th Annual AIAA/BMDO Technology Readiness Conference, Eglin AFB, September 16–20, 1996.

31. See S. H. Chen, *Control Forces Produced By Lateral Jet Injection*, Aerospace Corporation, Aerospace Technical Memorandum No. 92(2031-01)-1, January 1992.

32. See, for example, Paul Zarchan, *Tactical and Strategic Missile Guidance*, Volume 176, Progress In Astronautics and Aeronautics, American Institute of Astronautics and Aeronautics, 1997, pp. 291–316.

33. See *Boost-Phase Intercept Systems for National Missile Defense*, op. cit., Sections 12.2.4; and L.C. Ng, E. Breitfeller, and A.G. Ledebuhr, *An Optimal  $t-\Delta V$  Guidance Law for Intercepting a Boosting Target*, Lawrence Livermore National Laboratory, UCRL-JC-148995, June 30, 2002.

34. See *Boost-Phase Intercept Systems for National Missile Defense*, op. cit., Section 12.3.

35. *Boost-Phase Intercept Systems for National Missile Defense*, op. cit., Sections 12.3.2 and 12.4.

36. No clear advantage occurs for second versus third stage maneuvering in Figure 7 because lower KKV acceleration is required over a longer time to correct for second stage maneuvers compared to higher acceleration over shorter periods for diverts that come later in the booster's flight.

37. The SRAM-A, Air-Launched Cruise Missile, and Advanced Cruise Missile have masses of 1,012 kg, 1,458 kg, and 1,250 kg, respectively. See Duncan Lennox, *Jane's Strategic Weapon Systems*, Issue 32, Jane's Information Group, UK, 2000. Fighter aircraft carry about two to five 2,000 lb bombs. See Jane's *All The World's Aircraft*, Jane's Information Group, UK, 1993, pp. 408, 410.

38. These ABI designs have axial accelerations of approximately 50 g. The highest acceleration ground-based interceptor ever developed by the United States was the nuclear-tipped Sprint missile defense interceptor with a nominal axial acceleration of about 100 g (see <http://www.designation-systems.net/dusrm/app4/sprint.html>) (29 March 2004). This missile required ablative coatings to handle the atmospheric heating. The ABIs shown in Table 4 have much lower atmospheric heating because they are launched at high altitudes and, hence, require only a simple shroud to protect the KKV during flight.

39. See Kevin Bell, David Johannsen, and Kevin Zondervan (Aerospace Corporation), Major Samuel Walker (Air Force Space and Missile Systems Center), Paul Fry, Robert Hintz and Patrick Yates (Naval Air Warfare Center, China Lake), "An Airborne Interceptor for Boost Phase and Early Midcourse Theater Missile Defense," paper presented at the 1994 BMDO Intercept Technology Conference, 1994.

40. See Douglas Moody, *COMET: Calculation of Missile Earth Trajectories*, 2nd Ed., RAND Corporation, R-3240-1-DARPA/BMDO/RC, February 1997.

41. This is the 2002 release of a semitheoretical, semiempirical aerodynamic prediction code designed by Dr. Frank G. Moore, API Incorporated, King George, VA.

42. The intercept zone is a circle because ABIs lose relatively little range even if they execute a 180-degree turn shortly after launch to head toward their intercept point. Note that the zone on the ground from which missile launches can be intercepted is a more complicated shape and depends on the spread in azimuth for the missile launches from a particular launch site.

43. For the B1B bomber cost see ([http://www.af.mil/news/factsheets/B\\_1B\\_Lancer.html](http://www.af.mil/news/factsheets/B_1B_Lancer.html)) (29 March 2004); for the F-15, F-16, and F-18 fighter costs see ([http://www.af.mil/news/factsheets/F\\_15\\_Eagle.html](http://www.af.mil/news/factsheets/F_15_Eagle.html)) (29 March 2004), ([http://www.af.mil/news/factsheets/F\\_16\\_Fighting\\_Falcon.html](http://www.af.mil/news/factsheets/F_16_Fighting_Falcon.html)) (29 March 2004), and (<http://www.chinfo.navy.mil/navpalib/factfile/aircraft/air-fa18html>) (29 March 2004); and for the Global Hawk UAV

cost see ([http://www.fas.org/irp/program/collect/docs/man-ipc-global\\_hawk-010322.htm](http://www.fas.org/irp/program/collect/docs/man-ipc-global_hawk-010322.htm)) (June 2003).

44. One example of a fractionated kill vehicle design is given in A.G. Ledebuhr, et al., *Genius Sand: A Miniature Kill Vehicle Technology to Support Boost-phase Intercepts and Midcourse Engagements*, Lawrence Livermore National Laboratory, UCRL-JC-148992, June 30, 2002.

45. Anti-submarine warfare sensors may localize submarines to some extent. However, the United States would still face the daunting challenge of maintaining airborne platforms above possible SLBM launch locations far from ABI support bases for long periods of time.

46. *Boost-Phase Intercept Systems for National Missile Defense*, op. cit., p. xxv–xxvi.

47. The present study also made several assumptions that reduce the ABI intercept range relative to the APS results, namely, assuming lofted ICBM trajectories and requiring that the intercept occur far enough in advance of the nominal boost time to account for 5 percent fluctuations in the missile's burn time.

48. Lofting or depressing the trajectory is assumed to occur with the missile's second stage. Minimum energy trajectories use premature thrust termination so the payload has sufficient speed just to reach the target.

49. When a booster is intercepted its thrust should drop to zero quickly due to the booster's collapse. The resulting forces will scatter missile debris in a roughly elliptical zone as opposed to a single point on the Earth's surface. The size of this elliptical impact zone will depend on the velocity imparted to the various fragments during the impact. Some of this debris will burn up upon reentry into the earth's atmosphere. However, the remainder may scatter over a wide area with large pieces, including possibly the intact payload, landing close to the ranges indicated in Figures A7 and A8.

## **APPENDIX A**

### **BALLISTIC MISSILE CHARACTERISTICS**

This Appendix describes the ballistic missile characteristics that are important for analyzing boost-phase ballistic missile defense effectiveness. Table A1 lists the characteristics of a variety of notional medium, intermediate, and intercontinental-range ballistic missiles that could pose a threat to U.S. forces overseas or the U.S. homeland. These estimates are based on open sources for missiles that actually exist (i.e., Scud B, Scud C, No Dong, and Taepo Dong 1 missiles). The Taepo Dong 2, Shahab 5, and the three ICBMs are notional designs that span a range of possible future intermediate- and intercontinental-range ballistic missile threats. The 2-stage liquid-propellant ICBM is designed to have a burn time of approximately 300 seconds—comparable to that of first generation U.S. and Soviet liquid-propellant ICBMs. With a launch weight of 110,000 kg, this missile has a nominal range of 11,500 km with a payload of 400 kg.

**Table A1:** Ballistic missile characteristics.

	Scud B	Scud C	No Dong	Taeпо Dong 1	Taeпо Dong 2	Shahab 5	290-sec ICBM	240-sec ICBM	180-sec ICBM
Nominal range (km)	300	610	1,340	1,920	3,680	4,750	10,700	10,700	14,500
Payload (kg)	985	700	1,000	1,000	1,000	500	400	300	800
Launch mass (kg)	5,900	7,200	20,000	25,400	69,000	70,500	110,000	69,000	45,800
Boost time (sec)	61	85	95	165	193	199	290	240	180
Max burnout speed (km/sec)	1.6	2.3	3.4	3.7	5.0	5.4	7.1	7.1	7.5
<b>1st Stage</b>									
Stage mass (kg)	4,915	6,500	19,000	19,000	50,000	52,000	95,000	50,000	29,000
Prop. fraction	0.72	0.77	0.85	0.85	0.82	0.83	0.87	0.82	0.89
CS area (m <sup>2</sup> )	0.61	0.61	1.13	1.13	4.52	4.52	3.14	4.52	2.0
Nozzle area (m <sup>2</sup> )	0.15	0.15	0.28	0.28	1.13	1.13	1.54	1.13	1.3
Vac. thrust (kN)	145	153	429	429	1,315	1,315	1,655	1,315	1,225
Vac. isp (sec)	257	267	257	257	263	263	293	263	291
Burn time (sec)	61	85	95	95	80	85	143	80	60
<b>2nd Stage</b>									
Stage mass (kg)	—	—	—	5,400	18,000	18,000	15,000	18,000	12,000
Prop. fraction	—	—	—	0.74	0.83	0.84	0.83	0.83	0.87
CS area (m <sup>2</sup> )	—	—	—	0.61	1.39	1.39	1.77	1.39	1.77
Nozzle area (m <sup>2</sup> )	—	—	—	0.15	0.35	0.35	0.44	0.35	0.87
Vac. thrust (kN)	—	—	—	145	350	350	240	350	495
Vac. isp (sec)	—	—	—	257	270	270	290	270	290
Burn time (sec)	—	—	—	70	113	114	147	113	60
<b>3rd Stage</b>									
Stage mass (kg)	—	—	—	—	—	—	—	700	4,000
Prop. fraction	—	—	—	—	—	—	—	0.80	0.84
CS area (m <sup>2</sup> )	—	—	—	—	—	—	—	0.61	1.54
Nozzle area (m <sup>2</sup> )	—	—	—	—	—	—	—	0.15	0.75
Vac thrust (kN)	—	—	—	—	—	—	—	30	160
Vac. isp (sec)	—	—	—	—	—	—	—	250	290
Burn time (sec)	—	—	—	—	—	—	—	47	60

Smaller missiles could achieve the same range with smaller payloads. However, modern liquid-propellant ICBMs (e.g., the Chinese DF-5) have boost times on the order of 230–250 seconds. To represent a missile of this class, Table A1 includes a 240-second ICBM, based in this case on the Taepo Dong 2 IRBM with a solid-propellant third stage to give it a range of approximately 11,500 km with a 300 kg payload—the assumed minimum payload for a small first generation nuclear (fission) weapon. Finally, the 180-second solid-propellant ICBM is modeled after the Russia SS-25 ICBM. The payload has been reduced from that of the SS-25 to give the missile sufficient range to strike the entire United States from launch locations in North Korea or Iran. This solid-propellant ICBM is included to reflect the impact of an obvious countermeasure to boost-phase missile defense, namely, shortening the boost time with faster burning solid-propellant rocket motors. How soon emerging missile states might acquire solid-propellant ICBMs is not clear, though it depends no doubt on the extent to which foreign assistance is forthcoming from more advanced missile states. For the purpose of this study, it has been assumed that emerging missile states cannot develop “fast-burn” solid-propellant ICBMs within the next decade or two with boost times on the order of 100–130 seconds, which were hypothesized as a Soviet responsive threat to U.S. space-based ballistic missile defenses in the mid-1980.

Figure A1 shows a range-altitude plot for the Scud B, Scud C, and No Dong boost phases. The Scud B burns out in 61 seconds at an altitude of about 27 km. The Scud C modeled in this analysis has a range of 615 km with a payload of 700 kg, a burn time of 85 seconds, and a burnout altitude of approximately 50 km. The No Dong burns out in 95 seconds at an altitude of approximately 70 km. Figure A2 illustrates intermediate-range, two-stage, Taepo Dong 1 and Taepo Dong 2 boost phases with nominal burn times of 165 and 193 seconds, and burnout altitudes of approximately 150 and 210 km, respectively, along with the three stage, 240-second ICBM with a burnout altitude of approximately 190 km for a maximum-range trajectory.

Figure A3 illustrates the variation in ICBM burnout altitudes that occur for lofted, minimum energy, and depressed trajectories against cities at different range from a North Korean launch location for the 240-second ICBM.<sup>48</sup> As one can see, burnout altitude variations are greater against targets at short ranges and for eastward trajectories (due to the larger component of the Earth’s rotational speed) because more propellant exists for lofting or depressing the trajectory. For example, North Korean launches against Anchorage, Alaska have the largest variation, while launches against Boston show the least. Note that the variation in burnout altitudes for ICBMs can be as large as 350 km.

Figure A4 illustrates the acceleration profiles for several medium and intermediate-range ballistic missiles. The No Dong has the highest peak

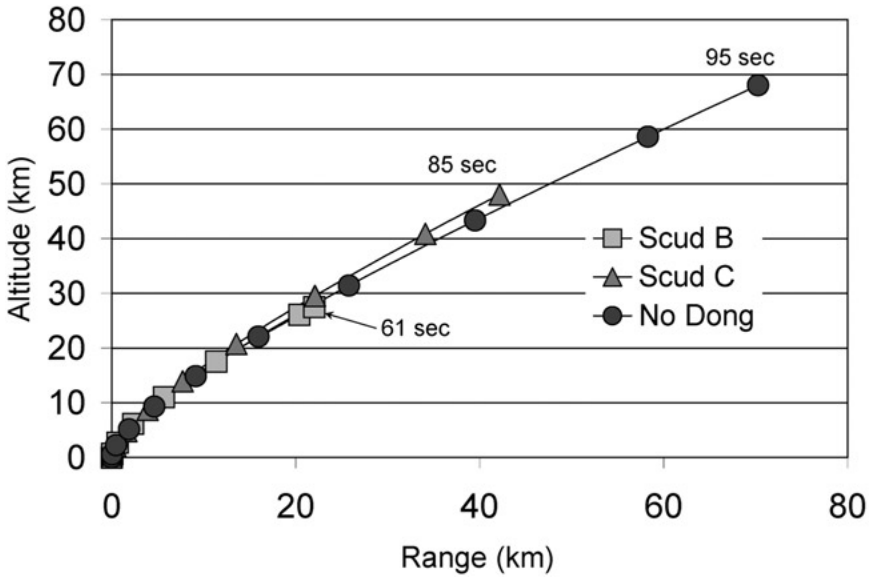


Figure A1: Scud B, Scud C, and no Dong boost phases.

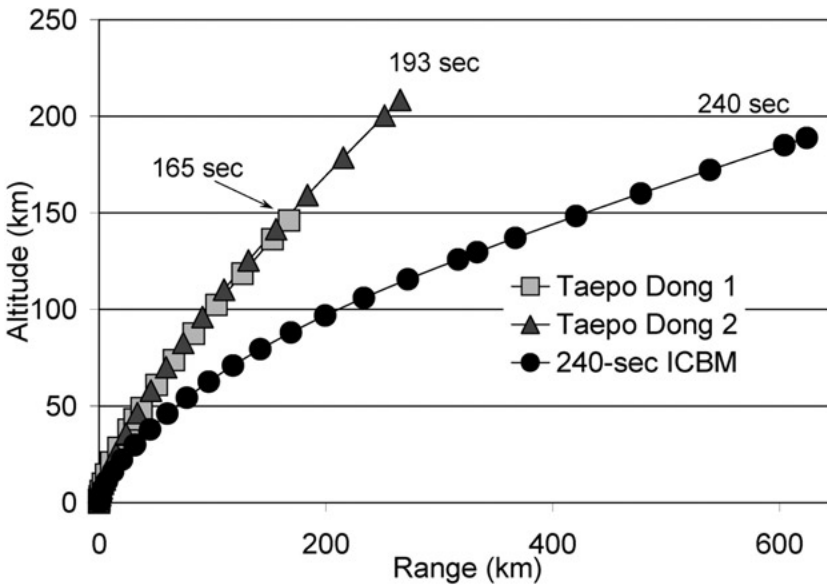


Figure A2: Taepo Dong 1, Taepo Dong 2, and ICBM boost phases.

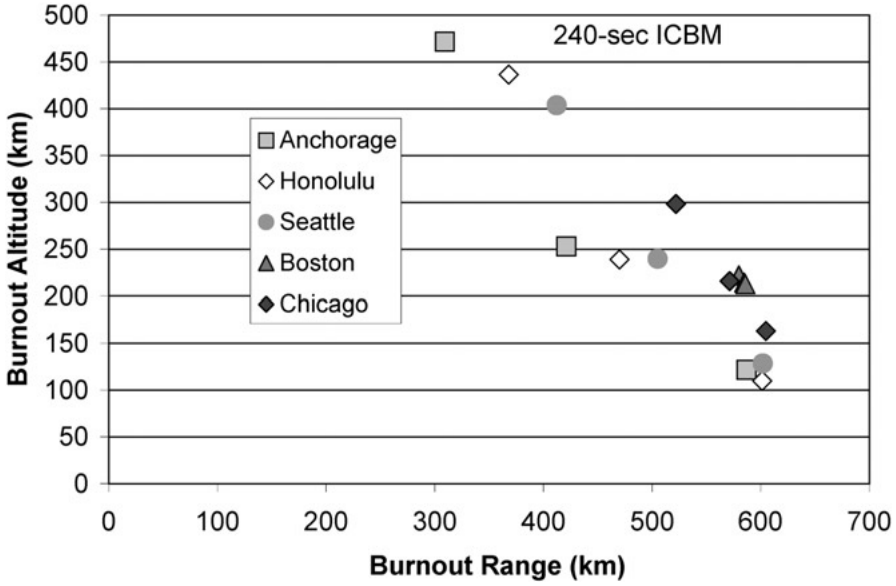


Figure A3: 240-sec ICBM burnout points for different trajectories.

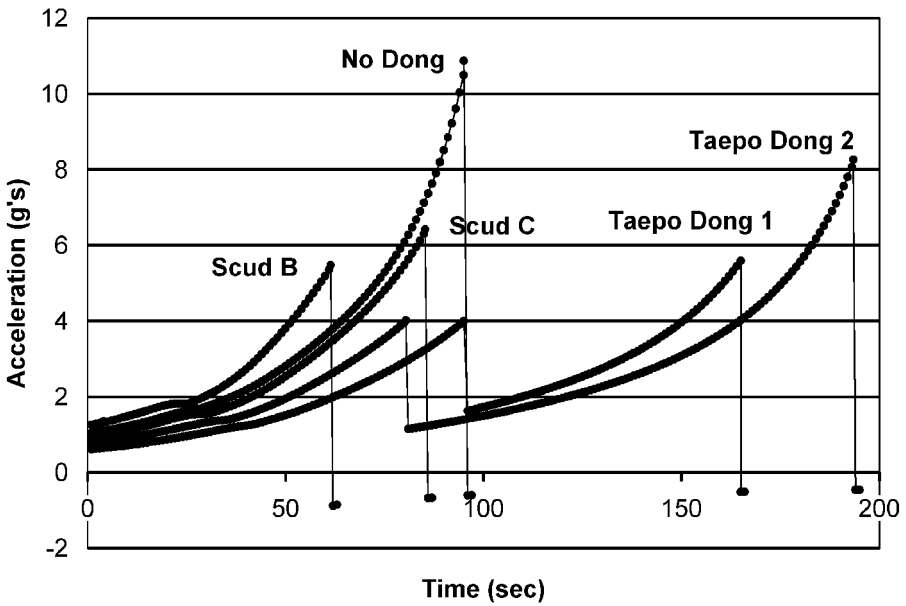


Figure A4: Acceleration profiles for medium-range ballistic missiles.



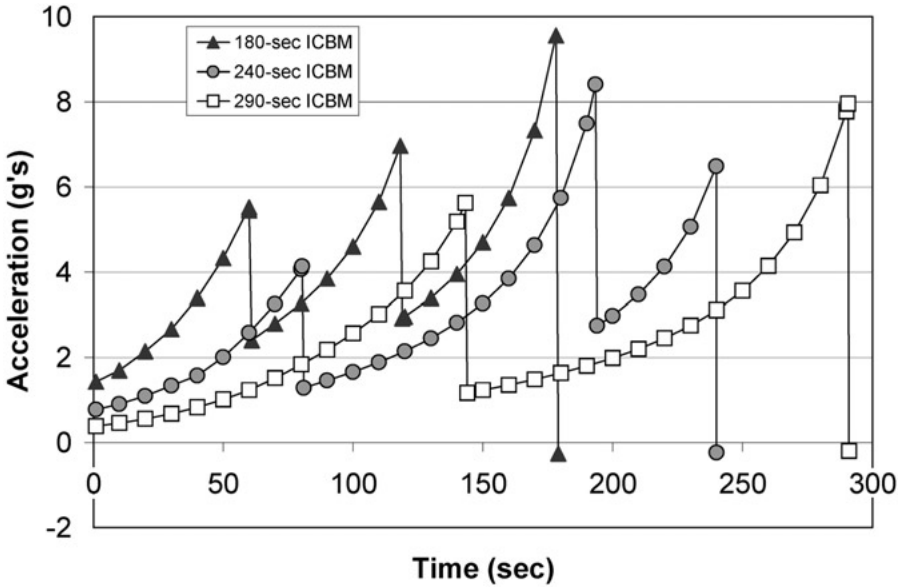


Figure A5: Acceleration profiles for ICBMs.

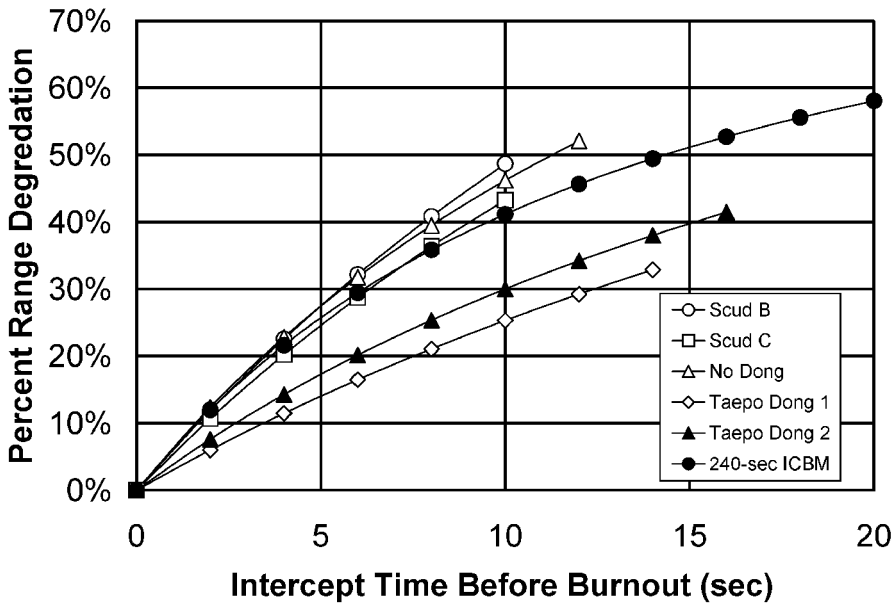
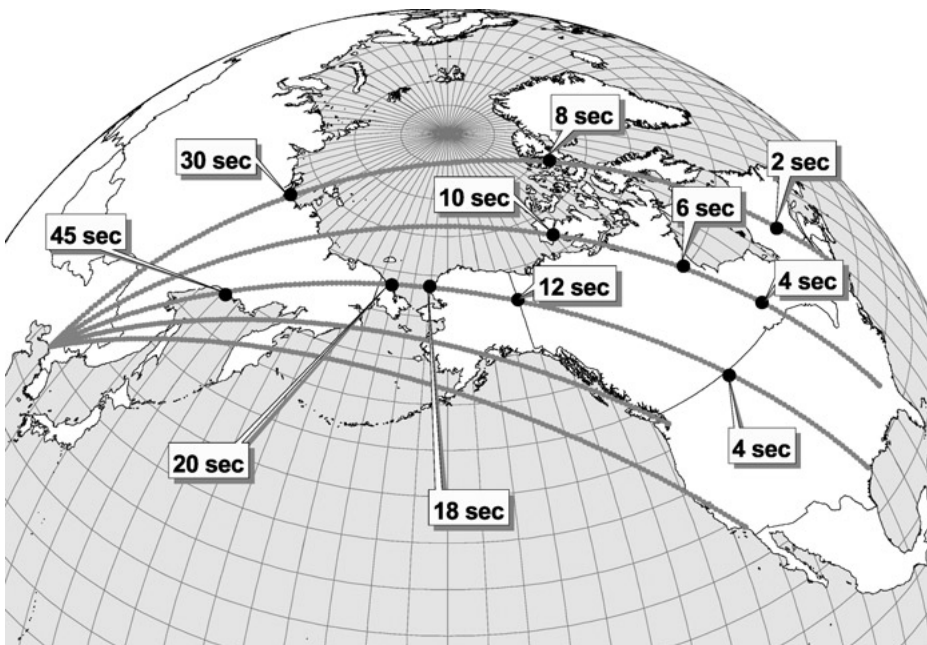


Figure A6: Missile range degradation vs. premature thrust termination.

acceleration among those modeled in this analysis, reaching nearly 11 g at its maximum. Typical accelerations several seconds before booster burnout are between 5 g and 6 g. Figure A5 illustrates the acceleration profile for the three ICBMs modeled in this analysis. While peak ICBM accelerations may reach 10 g, typical accelerations several seconds before burnout are in the range 6–8 g.

The high acceleration at the end of the boost phase imparts considerable velocity to the payload and, hence, contributes substantially to a missile's range, especially for intercontinental-range missiles due to the earth's curvature. Conversely, if a missile's thrust is terminated prematurely by several seconds, its range is degraded substantially. Figure A6 illustrates this range degradation as a function of the premature thrust termination in seconds. Terminating a ballistic missile's thrust prematurely by 5 seconds typically decreases its range by 15 to 30 percent.

Figures A7 and A8 illustrate the range shortfall for ICBM trajectories launched from North Korea and Iran, respectively, towards the United States. Intercepting North Korean or Iranian ICBMs two to four seconds before booster burnout causes the payload to fall north of the U.S.-Canadian border.<sup>49</sup>



**Figure A7:** North Korean ICBM trajectories toward the United States.

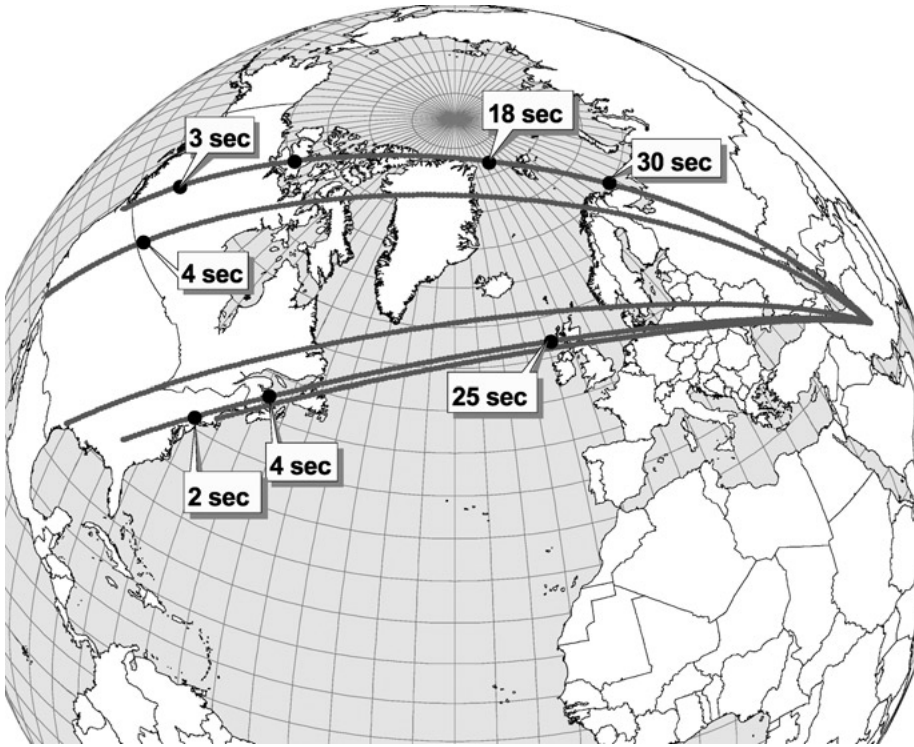


**Figure A8:** Iranian ICBM trajectories toward the United States.

Intercepting North Korean or Iranian ICBMs approximately 10 seconds before burnout ensures that the payload will fall short of North America, except for North Korean trajectories that pass over Alaska. Intercepts that occur 10 to 30 seconds before burnout would cause the payload to fall relatively harmlessly into the Arctic or North Atlantic Oceans, except for North Korean trajectories that pass over Alaska and Iranian trajectories that pass over Greenland. North Korean ICBMs intercepted more than 30 seconds before burnout would cause the debris to fall in Siberia. Similarly, Iranian ICBMs intercepted 25–30 seconds before burnout would cause the payload and debris to land in northern Russia or Europe. Given uncertainties in the exact ICBM burnout time (due to uncertainties in the exact launch time, physical variations in a missile’s burn rate, and trajectory variations) that cannot be eliminated prior to launching a boost-phase interceptor, it will be very difficult if not impossible to intercept the target booster within the narrow time window that guarantees that debris will not fall on friendly territory.